Academic Studies and New Visions in Engineering

Editor: Prof. Dr. Selmin ENER RÜŞEN

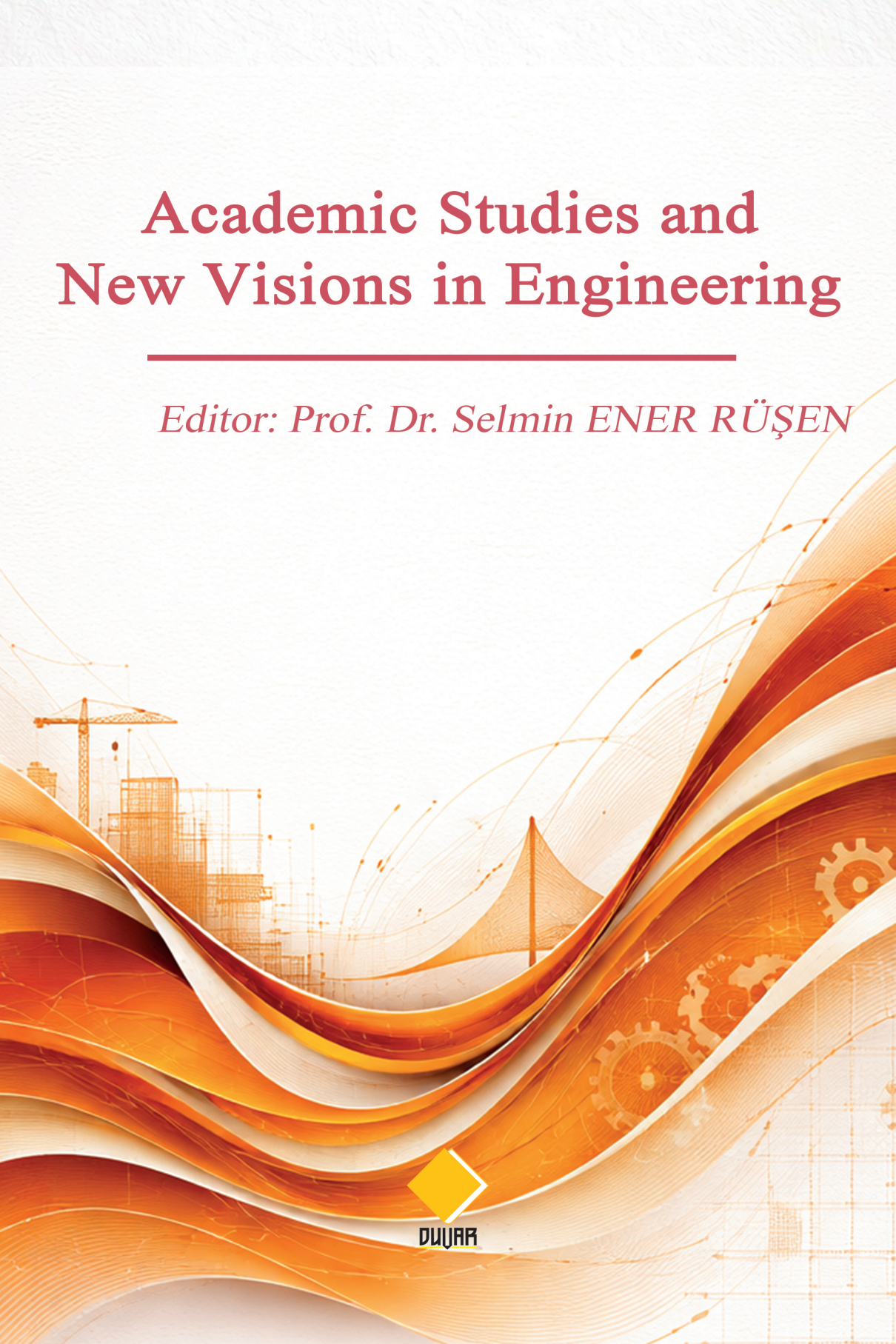

DUVAR

ACADEMIC STUDIES AND NEW VISIONS IN ENGINEERING

Editor

Prof. Dr. Selmin ENER RÜŞEN

Academic Studies And New Visions In Engineering
Editor: Prof. Dr. Selmin ENER RÜŞEN

Editor in chief: Berkan Balpetek
Cover and Page Design: Duvar Design
Printing : March -2026
Publisher Certificate No: 49837
E-ISBN: 978-625-8756-15-9

853 Sokak No:13 P.10 Kemeraltı-Konak/İzmir
Tel: 0 232 484 88 68
www.duvaryayinlari.com
duvarkitabevi@gmail.com

TABLE OF CONTENTS

Chapter 1

An Overview of Composite Boat Manufacturing Methods

Fatih BALIKOĞLU[1], Mehmet ÖZER[2]

ABSTRACT

The requirements for lightness, high rigidity, and corrosion resistance in marine structures have led to the widespread use of composite materials. This study comparatively examines hand lay-up, vacuum infusion (VARIM), resin transfer molding (RTM), and prepreg-autoclave production methods. The methods were evaluated in terms of fiber volume ratio, void ratio, mechanical performance, production cost, and suitability for mass production. Furthermore, bending rigidity, impact strength, and delamination behavior were analyzed specifically for boat hulls. In conclusion, while the vacuum infusion method offers an optimum performance-cost balance in medium and large-scale yacht production, the prepreg-autoclave method provides superior mechanical properties in high-performance racing and military platforms.

Keywords: Boat manufacturing**,** marine composites, sandwich panels.

1. INTRODUCTION

The application of fiber-reinforced polymer (FRP) materials in marine vessel construction emerged in the period following World War II and has evolved substantially over the subsequent decades. Prior to the 1950s, composite vessels were generally restricted to relatively small dimensions, typically below 15 meters in length and limited displacement capacities. However, advancements in material engineering, structural design methodologies, and manufacturing technologies enabled significant increases in hull size and load-bearing capability. As a result, lightweight composite structures are now widely utilized not only in recreational craft but also in naval platforms, including corvette-class vessels.

Initial large-scale implementation of composite materials occurred within military marine programs. After World War II, the United States Navy initiated the production of composite-based personnel boats. Numerous landing, reconnaissance, and patrol craft manufactured during this period were deployed in the Vietnam War.

[1] Doç. Dr. Balıkesir University, Faculty of Engineering, Department of Mechanical Engineering, Balıkesir, Turkiye, Orcid: 0000-0003-3836-5569

[2] Öğr. Gör. Dr. Balıkesir University, Bigadiç Vocational School, Department of Transportation Services Program, Balıkesir, Turkiye, Orcid: 0000-0002-6212-1217

These early applications catalyzed rapid expansion of composite boat manufacturing throughout the mid-20th century. During the 1960s, the commercial sector experienced substantial growth in FRP boat production, driven by low maintenance requirements and cost efficiency. The widespread accessibility of composite technology contributed to increased boat ownership and diversification of vessel classes (Mouritz, Gellert, Burchill, & Challis, 2001).

Today, composite materials are extensively utilized in both civilian and defense maritime sectors. In addition to leisure craft, medium-scale naval vessels—such as patrol boats, mine countermeasure units, and corvette-class ships—are increasingly constructed using advanced composite systems due to their superior strength-to-weight ratio and resistance to corrosive marine environments.

2. MARINE COMPOSITE PRODUCTION METHODS

Marine structures, particularly boat and yacht hulls, are exposed to complex service loads including hydrostatic pressure, wave-induced impact (slamming), global bending moments, and cyclic fatigue effects. In such demanding environments, fiber-reinforced polymer (FRP) composites are frequently selected over conventional metallic materials due to their superior specific stiffness and strength characteristics.

Sandwich composite configurations consist of two relatively thin, but mechanically strong face sheets bonded to a lightweight core material with greater thickness. Core materials commonly include PVC foam, PET foam, balsa wood, or engineered honeycomb structures. This structural arrangement enhances flexural rigidity significantly while maintaining low overall structural weight, making it particularly suitable for marine hull applications.

The selection of a suitable manufacturing technique in boat construction depends on multiple interrelated parameters, including production rate, economic constraints, structural strength requirements, as well as the geometric scale and complexity of the component. For large-scale structures such as hull shells, open-mold manufacturing techniques historically dominated the industry.

Early glass-reinforced plastic (GRP) boat constructions typically employed reinforced monocoque designs to maintain panel stability within acceptable dimensional limits. These early composite vessels were manufactured using isotropic glass fiber mats combined with orthophthalic polyester resins, primarily through manual lay-up or spray-up processes (Figure 1). From the 1960s onward, hand lay-up became the prevailing fabrication technique for small- and medium-sized boats and yachts. During the 1970s, the adoption of sandwich structures marked a significant technological advancement, improving stiffness-to-weight performance. By the 1990s, vacuum-assisted processes—including vacuum bagging

and resin infusion—were introduced into the marine sector, leading to improved laminate quality and reduced defect rates [(Greene, 1997; Neşer, 2017). Currently, resin infusion and hand lay-up processes are the most common techniques used by boat builders (Figure 2).

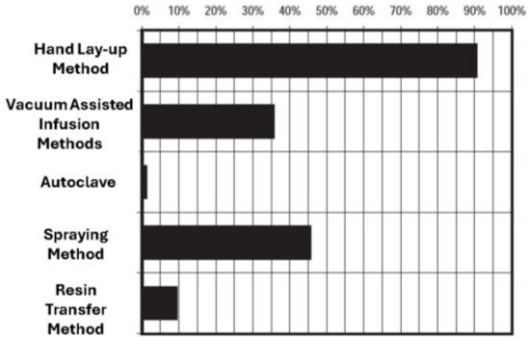

Figure 1. Preferred production methods in marine vessel production (Greene, 1997).

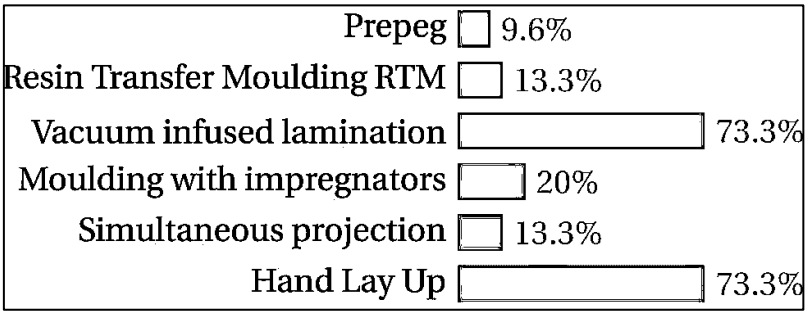

Figure 2. Survey results on EU shipyards (Dolz, Martinez, Sá, Silva, & Jurado, 2024).

2.1. HAND LAY-UP METHOD

As noted earlier, hand lay-up remains the most widely implemented manufacturing technique in composite boat construction. Both monolithic laminates and sandwich-structured composites can be fabricated using this method. Figure 3 illustrates a representative example of monocoque laminate deck production, while Figure 4 presents a schematic view of vessel fabrication through manual molding.

One of the most critical parameters affecting the structural integrity of sandwich composites produced by this method is void content. Voids are considered manufacturing-induced defects and may develop during resin mixing, impregnation, or curing stages. Additionally, moisture absorbed by the resin during storage or processing can contribute to porosity formation. Elevated void content reduces fatigue resistance and increases susceptibility to moisture ingress. For high-performance composite structures, the void fraction should ideally remain below 1%,

whereas values approaching 5% are generally indicative of lower-quality laminates. Furthermore, voids and foreign inclusions may occur at the skin–core interface, potentially initiating delamination under shear stresses generated during service loading. For this reason, hand lay-up operations must be carefully planned and executed efficiently, supported by adequate manpower and appropriate tooling, to minimize structural inconsistencies (Calabrese, Di Bella, & Fiore, 2016).

The production sequence of sandwich composites using the hand lay-up method typically involves the following steps (Calabrese et al., 2016; Mazumdar, 2001):

- Preparation of fiber reinforcements by cutting and labeling layers in accordance with mold dimensions and lamination schedules.
- Cleaning of the mold surface followed by the application of a suitable release agent.
- Application of gelcoat to the mold surface to form the exterior aesthetic and protective layer of the vessel.
- Placement of chopped strand mat or woven reinforcements according to the stacking sequence, followed by manual resin impregnation using brushes, rollers, or wetting tools. Successive layers are applied in a wet-on-wet manner without allowing intermediate curing.
- Positioning of the core material and application of resin to ensure bonding.
- Placement of the upper reinforcement layers over the core, followed by resin impregnation.
- Allowing the laminate to cure for approximately 24–48 hours, depending on resin type and environmental conditions.

Advantages of the Hand Lay-Up Method are listed below (Calabrese et al., 2016; Mazumdar, 2001)

- Requires relatively low capital investment and equipment cost.
- Utilizes simple molds and basic hand tools, facilitating ease of implementation.
- Offers flexibility in component size, with minimal geometric limitations.
- Provides significant design adaptability for complex shapes.
- Suitable for both monolithic laminates and sandwich composite structures.
- Effective for prototyping and gradual scaling of production.
- Economically viable for vessels shorter than approximately 24 meters.
- Appropriate for low-to-medium production volumes (approximately 50–100 units per month).

Disadvantages of the Hand Lay-Up Method are listed below (Calabrese et al., 2016; Mazumdar, 2001)

- Surface finish quality is achieved on only one side due to the open-mold configuration.
- Strongly dependent on operator skill and experience.
- May result in non-uniform resin distribution, including dry spots or resin-rich regions.
- Limited control over laminate thickness, fiber volume fraction, and porosity levels.
- Generates significant styrene emissions during curing, necessitating adequate ventilation systems.
- Requires strict use of personal protective equipment and environmental safety measures in shipyard operations.

Figure 3. Boat manufacturing by hand lay-up method (Güven Tekne Ltd. Şti, Çiğli, İzmir), a) Female polyester hull mold, b, c) Fiberglass lay-up, d) Resin impregnation.

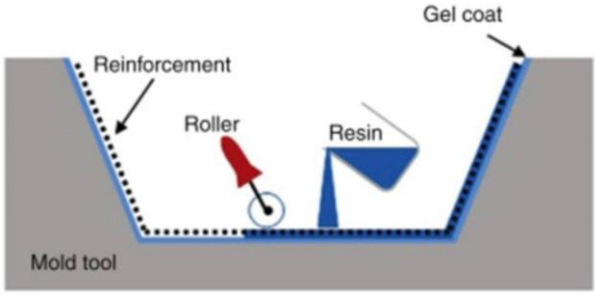

Figure 4. Schematic representation of boat building using the hand lay-up method (Middleton, 2015).

2.2. VACUUM-BASED COMPOSITE MANUFACTURING TECHNIQUES

Limitations associated with conventional open-mold manufacturing techniques have encouraged the development of vacuum-based composite processing technologies. Among these are vacuum bagging (VB) and various resin infusion techniques such as VARIM, SCRIMP, RIFT, and related systems.

Vacuum based techniques offer several technical advantages. Firstly, entrapped air between wet layers is effectively removed, reducing void formation. Secondly, applied compaction pressure improves interlaminar bonding and helps prevent fiber misalignment during curing. Thirdly, evacuation of air and moisture decreases porosity and limits moisture absorption within the final structure. Additionally, resin distribution becomes more uniform, minimizing dry spots and resin-rich areas. Since surplus resin is absorbed by the breather layer, the fiber-to-resin ratio improves compared to conventional hand lay-up laminates. As a result, composites manufactured by vacuum bagging typically exhibit lower void content, reduced weight, enhanced mechanical performance, improved thickness consistency, and higher fiber volume fraction relative to open-mold processes (Calabrese et al., 2016; Karlsson & TomasÅström, 1997).

2.2.1. Resin Infusion

The Seemann Composite Resin Infusion Molding Process (SCRIMP), introduced by Bill Seemann in 1990, represents a closed-mold composite manufacturing technique that has gained widespread industrial adoption, particularly in the United States.

This technology is described in the literature using various designations and abbreviations, including VARTM, RIF, SCRIMP, RFI, RFIM, VAIM, VARI, VARIM, VIM, and VIMP. Among these, Resin Infusion under Flexible Tooling (RIFT) and SCRIMP are the most referenced terms (Marsh, 2010; Summerscales & Searle, 2005). Despite terminological variations, the fundamental principle remains consistent: resin is introduced into a dry reinforcement preform under vacuum within a sealed mold environment.

The VARIM technique, extensively applied in marine composite production, is classified as a closed-mold resin infusion process and shares similarities with Resin Transfer Molding (RTM). However, unlike conventional RTM systems that employ two rigid mold halves, VARIM utilizes a single rigid mold sealed with a vacuum bag to establish a controlled infusion environment.

A primary distinction between VARIM and traditional vacuum bagging lies in the placement of materials. In VARIM, dry reinforcement fabrics and core materials are arranged directly inside the mold before resin is introduced. Therefore, no preliminary wet lay-up stage is required. Vacuum pressure performs a dual function

in this method: it compacts the reinforcement stack while simultaneously enabling resin flow through the laminate. As a result, once the preparation phase is completed, impregnation progresses without continuous manual application.

In VARIM applications, a flow media layer (flow mesh) is generally positioned above the peel-ply to enhance resin distribution and shorten filling time. The system typically consists of several components, including mold, spiral distribution hoses, T-connections, resin inlet lines, vacuum lines, sealing tapes, a vacuum pump, a resin trap, and a resin supply tank (Figure 5).

In practical terms, the infusion mechanism allows resin to travel from designated feed lines toward vacuum outlets within the sealed mold cavity. Depending on part geometry and process strategy, feed lines may be arranged centrally, linearly, or circumferentially. The configuration of resin and vacuum networks significantly influences filling behavior and total production duration. Moreover, the absolute pressure differential applied across the system directly affects resin flow characteristics and final laminate quality.

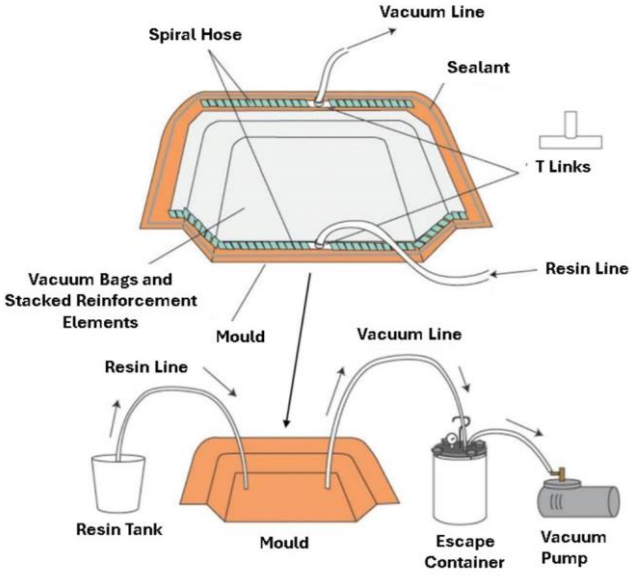

Figure 5. VARIM production facility (Calabrese et al., 2016).

In the VARIM process, appropriate selection of resin and reinforcement materials is essential. Generally, low-viscosity resins are preferred because they penetrate reinforcement layers more efficiently. Infusion-specific resin systems are widely available; however, higher-viscosity resins may also be employed provided that the process is carefully designed, often requiring additional or shorter resin distribution lines.

Reinforcement selection is also critical for composite performance. Although the infusion method can theoretically be applied to various textile forms, fabric architecture strongly influences resin permeability. Resin advancement tends to be more efficient in woven fabrics due to fewer fiber interlacements. Knitted fabrics and chopped strand mats typically absorb higher resin volumes. In contrast, stitched non-crimp fabrics generally exhibit lower resin absorption rates.

It must also be considered during design that many reinforcement systems can experience thickness reductions of up to approximately 30% under vacuum pressure. Core material selection is equally important. Closed-cell core materials are generally recommended for VARIM, whereas open-cell honeycomb cores are less suitable due to uncontrolled resin uptake. To improve resin flow, grooves, perforations, or channels may be introduced into core materials, enabling sufficient permeability and bonding. Such modifications make it possible to manufacture sandwich composites even with reduced reliance on flow media layers. Several core manufacturers (e.g., DIAB, Airex, Baltek) provide modified core products designed to enhance resin transfer performance according to specific application requirements (Reuterloev, 2003; Reuterlöv, 2002). Figure 6 and 7 presents a schematic illustration of sandwich composite production using the VARIM technique and production of sandwich composite boat hull, followed by detailed explanation of the processing stages.

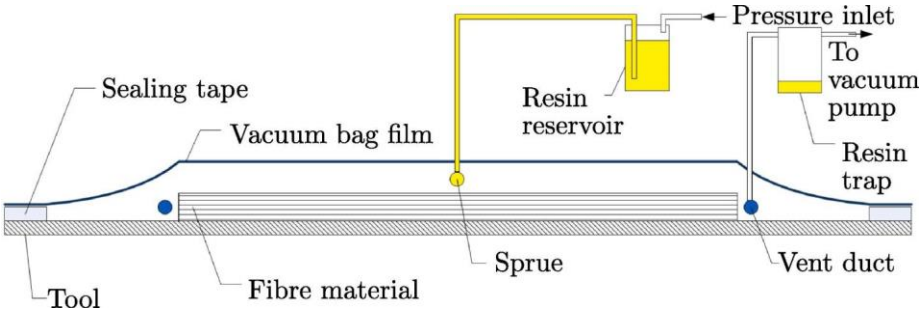

Figure 6. Production of sandwich composite boat hulls with VARIM (Hindersmann, 2019)

Figure 7. Production of sandwich composite boat hulls with VARIM (Technology update: Vacuum infusion,2004)

The manufacturing of sandwich composites via the VARIM process involves the following sequential operations:

- Fiber reinforcement layers are pre-cut and labeled on a workbench in accordance with the mold dimensions and lamination schedule.
- The mold surface is thoroughly cleaned, and an appropriate mold release agent is applied to ensure proper demolding after curing.
- Dry reinforcement fabrics and core materials are positioned inside the mold following the defined stacking sequence.
- Spiral distribution hoses for both resin inlet and vacuum outlet lines are prepared and placed inside the mold. T-connectors are attached to the spiral hoses to connect resin feed and vacuum lines. A double-sided sealing tape is applied along the mold perimeter to ensure airtight sealing.
- The vacuum bag is cut according to mold depth and laminate thickness to allow adequate compaction pressure during infusion. After trimming, the vacuum bag is fixed around the mold using sealant tape to create a closed system.
- Polyethylene hoses for resin feed and vacuum extraction are connected to the spiral distribution lines via T-connectors. The vacuum line is attached to the resin trap (escape container), while the resin feed line remains closed at this

stage. System integrity is verified by monitoring the pressure gauges on both the vacuum pump and the resin trap to detect possible leakage.

- The required resin quantity is calculated based on the lamination schedule, considering the expected resin retention within hoses and distribution lines.
- Hardener and accelerator components are added to the resin in the prescribed proportions and thoroughly mixed to ensure homogeneous curing behavior.
- The resin inlet valve is opened to initiate infusion. Once the reinforcement stack and core materials are fully impregnated, the resin inlet is closed.
- The sandwich composite is then allowed to cure either under ambient conditions or through controlled thermal curing, depending on the resin system specifications.

During the visit to GCG Yacht Manufacturing Ltd. Co. (Gaziemir / Izmir), the production stages of the sandwich composite panel produced using the VARIM production technique are given in Figure 8.

Figure 8. VARIM production stages of sandwich composite material (GCG Yacht Manufacturing Industry Inc., Sarnıç, İzmir), a) Placement of glass Fiber and foam materials into the mold b) pulling of spiral hoses, c, d) Installation of resin and vacuum hoses, e) Placement of vacuum nylon, f) Applying sealing paste, g, h) Opening of resin feeding line and resin impregnation.

The advantages of the VARIM method can be summarized as follows(Calabrese et al., 2016; Pemberton, Summerscales, & Graham-Jones, 2018; Summerscales & Searle, 2005):

- Enables a relatively high fiber-to-resin ratio (approximately 70/30), resulting in lightweight, mechanically robust, and rigid composite structures.
- Ensures low void content (typically below 1%), thereby decreasing the probability of crack initiation and structural damage.

- Minimizes the occurrence of resin-rich and dry zones, promoting uniform resin distribution throughout the laminate.
- Generates reduced styrene emissions compared to open-mold techniques. Emission limits generally range between 20 ppm and 100 ppm in European countries, with an average value of approximately 35 ppm in the USA.
- Eliminates the need for manual wet lay-up operations, contributing to reduced material waste and improved resin efficiency.
- Unlike processes limited by resin gel time, the reinforcement layers are positioned dry within the mold, avoiding time constraints associated with premature curing.
- Reduces manufacturing defects; excessive exothermic reactions caused by resin-rich areas are minimized, and dimensional distortion (warping) is less likely to occur.
- Produces repeatable laminate characteristics. Process parameters such as vacuum pressure and resin viscosity can be monitored and adjusted. Operators primarily focus on correct layer placement and fiber orientation according to the lamination plan.

Although VARIM offers considerable advantages compared to open-mold techniques, several critical considerations must be addressed (Calabrese et al., 2016; Pemberton et al., 2018; Summerscales & Searle, 2005):

- Personnel involved in infusion processes require specific training. They must be familiar with infusion consumables and equipment and capable of accurately interpreting lamination schedules.
- The number of process parameters requiring control is greater than in open-mold manufacturing. Environmental factors such as workshop temperature and humidity, fiber mass, resin composition, hardener and accelerator ratios, and mold temperature must be carefully regulated. Additionally, resin viscosity and vacuum pressure levels must be continuously monitored throughout infusion.
- Initial investment and operating costs are generally higher than those of open-mold methods. Numerous consumables and equipment components—including vacuum pumps, resin traps (escape vessels), vacuum bags, sealing materials, spiral and straight hoses—are required.
- Open-mold processing involves comparatively lower operational risk. In VARIM, once resin transfer has begun, the process cannot be reversed. A drop in vacuum pressure (e.g., due to power failure) or improper resin preparation may necessitate termination of production.

- Strict attention must be given to preventing air leakage within the mold and vacuum bag system.
- While VARIM can be applied to components of various sizes, it is not typically preferred for small, highly complex geometries. It is more suitable for large structural components—such as boat hulls—that must be produced efficiently within limited time frames.
- Determining optimal resin and vacuum line placement through trial-and-error can be costly. For this reason, infusion simulations are often conducted using commercial finite element software such as PAM-RTM, LIMS, PolyWorx, and myRTM. Furthermore, dedicated infusion test setups have been developed to control process parameters and obtain preliminary experimental data, thereby reducing the likelihood of failure during early production stages.

Today, a significant portion of yacht and boat manufacturers have adopted resin infusion production techniques to improve product quality, speed up the production process, and comply with stricter health and safety regulations. All indicators show that this trend will gain momentum and open mold techniques will be abandoned. This situation was also observed during the visits to the sector within the scope of the study. It was personally seen that the VARIM technique was preferred in shipyards where sandwich-structure yachts are produced.

2.3. RESIN TRANSFER MOLDING (RTM)

The RTM (Resin Transfer Molding) technology is a closed mold choice for composite manufacture, especially for marine boat parts needing good surface quality. This method uses glass fiber or carbon fiber reinforcing components and pressure to introduce resin into the mold after closing. The resin cures by thoroughly impregnating the fibers, creating a robust composite. Marine boats employ RTM to make deck pieces, hatches, internal structural elements, and equipment components. High surface quality, fiber-resin ratio control, and minimal environmental emissions are benefits of the process. The mold's high cost and difficulty attaching it to big boat hulls are drawbacks (Lee, Jung, & Park, 2021).

2.4. PREPREG AUTOCLAVE

The prepreg + autoclave method is a cutting-edge approach for producing high-performance composite structures. This technique uses vacuum bagging to insert pre-impregnated, partly cured, fiber-reinforced pre-prepared strips (prepreg) in a mold and autoclave it. Curing in the autoclave at high temperature and pressure produces composite components with excellent strength, light weight, and low void ratio. Racing boats, high-performance yachts, and military maritime vessels employ

this strategy. Although the prepreg + autoclave approach produces high-quality structures and mechanical strength, its utilization is restricted by high production costs and the requirement for specialized equipment (Dewangan & Chakladar, 2024; Ekuase, Anjum, Eze, & Okoli, 2022).

2.5. SPRAY-UP.

The spray-up open-mold approach is popular in composite boat construction. Fiberglass is chopped using a special spray cannon and sprayed onto the mold with resin. Air spaces are eliminated by roller compression, and the process continues until the appropriate thickness is reached. Spray-up is favored for mass-producing small and medium-sized fiberglass boats, fishing boats, and dinghies. Its speed, cheap labor costs, and mass production adaptability are its key benefits. Its limitations include the inability to adjust fiber orientation and poorer mechanical strength than more modern approaches (Assunção, Velasques, Zakrzevski, & Costa, 2024; Chirayil et al., 2023).

3. COMPARISON OF BOAT BUILDING METHODS

The selection of an appropriate manufacturing method for marine sandwich composite structures is primarily determined by structural performance requirements, economic considerations, production capacity, and quality assurance standards. In hull applications, the following evaluations can be made:

- The vacuum infusion technique represents an optimal balance between mechanical performance and cost efficiency for medium-scale commercial yacht manufacturing.
- The prepreg–autoclave process is more suitable for applications requiring superior mechanical performance and strict weight optimization, particularly in high-performance marine and specialized platforms.
- The hand lay-up method continues to be a viable option for low-budget and small-scale production environments.
- Looking forward, increasing environmental regulations and the development of sustainable resin systems are expected to play a decisive role in shaping future composite manufacturing strategies.

Table 1. Comparison of production methods.

Criteria	Open Molds	Vacuum Infusion (VARIM)	RTM	Prepreg + Autoclave
Investment Cost	Low	Medium	High	Very high
Labor Dependence	Very high	Medium	Low	Low
Fiber Volume Ratio	%30–40	%45–60	%50–60	%60–70
Void Ratio	High	Low	Very low	Very low
Mechanical Performance	Medium	High	High	Very high
Surface Quality	Medium	Good	Very good	Very good
Suitability for Mass Production	Low	Medium	High	Low
Environmental Emissions	High	Low	Low	Very low
Large Part Production	Suitable	Very suitable	Limited	Limited
Widespread Application in Marine Environments	Small boats	Modern yachts	Mass production parts	Racing/military platform

REFERENCES

Assunção, G. S. C., Velasques, J. A., Zakrzevski, A., & Costa, I. d. (2024). Mechanical properties of glass-fiber reinforced polyester composites manufactured by two different spray-up techniques. *Matéria (Rio de Janeiro), 29*(3), e20240450.

Calabrese, L., Di Bella, G., & Fiore, V. (2016). Manufacture of marine composite sandwich structures *Marine Applications of Advanced Fibre-Reinforced Composites* (pp. 57-78): Elsevier.

Chirayil, C. J., Peter, B., George, L., Jorly, A., Jipson, S., Varghese, A., & Thomas, S. (2023). Processing methods of unsaturated polyester *Applications of Unsaturated Polyester Resins* (pp. 71-89): Elsevier.

Dewangan, B., & Chakladar, N. (2024). Influence of out-of-autoclave and autoclave manufacturing processes on mechanical properties of glass fiber-reinforced epoxy composite. *Polymer Composites, 45*(17), 15998-16020.

Dolz, M., Martinez, X., Sá, D., Silva, J., & Jurado, A. (2024). Composite materials, technologies and manufacturing: Current scenario of European Union shipyards. *Ships and Offshore Structures, 19*(8), 1157-1172.

Ekuase, O. A., Anjum, N., Eze, V. O., & Okoli, O. I. (2022). A review on the out-of-autoclave process for composite manufacturing. *Journal of Composites Science, 6*(6), 172.

Greene, E. (1997). Design guide for marine applications of composites.

Hindersmann, A. (2019). Confusion about infusion: An overview of infusion processes. *Composites Part A: Applied Science and Manufacturing, 126*, 105583.

Karlsson, K. F., & TomasÅström, B. (1997). Manufacturing and applications of structural sandwich components. *Composites Part A: Applied Science and Manufacturing, 28*(2), 97-111.

Lee, H., Jung, K., & Park, H. (2021). Study on structural design and analysis of composite boat hull manufactured by resin infusion simulation. *Materials, 14*(20), 5918.

Marsh, G. (2010). Marine composites—drawbacks and successes. *Reinforced Plastics, 54*(4), 18-22.

Mazumdar, S. (2001). *Composites manufacturing: materials, product, and process engineering*: CrC press.

Middleton, B. (2015). Composites: manufacture and application. *Design and manufacture of plastic components for multifunctionality*, 53-101.

Mouritz, A., Gellert, E., Burchill, P., & Challis, K. (2001). Review of advanced composite structures for naval ships and submarines. *Composite Structures, 53*(1), 21-42.

Neşer, G. (2017). Polymer based composites in marine use: history and future trends. *Procedia engineering, 194*, 19-24.

Pemberton, R., Summerscales, J., & Graham-Jones, J. (2018). *Marine composites: design and performance*: Woodhead Publishing.

Reuterloev, S. (2003). Grooved Core Materials Aid Resin Infusion- Influence on Mechanical Properties. *SAMPE journal, 39*(6), 57-64.

Reuterlöv, S. (2002). Cost effective infusion of sandwich composites for marine applications. *Reinforced Plastics, 46*(12), 30-34.

Summerscales, J., & Searle, T. (2005). Low-pressure (vacuum infusion) techniques for moulding large composite structures. *Proceedings of the Institution of Mechanical Engineers, Part L: Journal of Materials: Design and Applications, 219*(1), 45-58.

Technology update: Vacuum infusion. (2004). Reinforced Plastics, 48(1), 28–29.

Chapter 1

Laser Surface Hardening: Principles, Developments, and Industrial Applications

Semih DURAN[1], Tevfik Oğuzhan ERGÜDER[2]

Abstract

Laser surface hardening (LSH) is a surface-treatment technique commonly used to improve the surface conditions of metallic materials without modifying their bulk properties. By irradiating the material surface using a high-energy laser beam, this process induces local heat to cause a rapid self-quenching of the newly formed hardened layer. One of the main advantages with LSH is that it enhances the hardness, wear resistance and fatigue properties without any subsequent distortion or size change in the part. Moreover, as a non-contact and highly controllable method, LSH offers precise localization and minimal heat-affected zones, which makes it highly attractive for modern industrial applications.

In recent years, the development of laser technologies and advancements in material science have further expanded the potential of LSH applications across various industries such as automotive, aerospace, energy, biomedical, and tool manufacturing. The process parameters, including laser power, scanning speed, hatch spacing, beam diameter, and interaction time, critically affect the microstructural evolution, such as the formation of martensitic phases or grain refinement, which directly influences the mechanical performance of the hardened layer. Additionally, the choice of substrate material plays a important role in determining the achievable surface characteristics. This chapter presents a comprehensive overview of LSH, highlighting the fundamental principles, process parameters, microstructural mechanisms, and property enhancements, supported by selected studies and recent research findings. It aims to provide researchers, engineers, and practitioners with an in-depth understanding of LSH as a versatile and efficient surface engineering technique for high-performance applications.

Keywords: LSH, wear resistance, hardness, microstructure

[1] Asst. Prof., Kafkas University, Faculty of Engineering and Architecture, Department of Mechanical Engineering, semih.duran@kafkas.edu.tr, ORCID: 0000-0001-7107-1461

[2] Asst. Prof., Kafkas University, Faculty of Engineering and Architecture, Department of Mechanical Engineering, oguzhan.erguder@kafkas.edu.tr, ORCID: 0000-0002-8876-6152

1. Introduction

Surface engineering is a multidisciplinary and rapidly evolving field that focuses on the modification and enhancement of material surfaces to improve their functional performance, durability, and resistance to environmental and mechanical degradation. The surface of a material component serves as the primary interface between the part and its operational environment, making it highly susceptible to wear, corrosion, fatigue, and other failure mechanisms. Given that many engineering failures originate at the surface, improvement of surface properties without adversely affecting the bulk characteristics is a critical goal for material scientists and engineers. This selective approach allows components to retain desirable core properties such as toughness, ductility, and strength while significantly enhancing surface hardness, wear and corrosion resistance (Cui et al., 2015; Guarino et al., 2017; Kusinski et al., 2012; B. Wang, Barber, et al., 2020; B. Wang, Pan, Liu, Barber, et al., 2020)

Over the past several decades, a diverse array of surface modification technologies has been developed, encompassing mechanical, chemical, thermal, and physical methods. These include processes such as shot peening, chemical vapor deposition (CVD), physical vapor deposition (PVD), carburizing, nitriding, induction hardening, and more recently, laser-based treatments. Each technique offers unique advantages and challenges related to process complexity, cost, environmental impact, and applicability to different materials and geometries. Among these, surface hardening techniques stand out due to their ability to markedly improve surface hardness and tribological properties, which are essential in components subjected to cyclic loading, abrasive wear, and fatigue conditions. The challenge lies in achieving these improvements without compromising the inherent toughness and ductility of the substrate material, thereby prolonging the service life of the components and reducing maintenance costs (Chen et al., 2018; Duan et al., 2023; Łach, 2024; Wagh et al., 2020).

In recent years, laser-based surface treatments have gained significant traction in both academic research and industrial applications owing to their superior precision, repeatability, and environmental friendliness. Laser surface hardening (LSH) specifically uses the high energy density and controllability of laser beams to rapidly heat the surface layer of metallic components above critical transformation temperatures, followed by rapid cooling that transforms the microstructure into hard phases such as martensite. This process allows for localized hardening with minimal distortion, reduced heat-affected zones, and compatibility with complex geometries. The rapid advancements in laser technology, including improvements in laser beam quality, power modulation, and scanning control, have further expanded the applicability and effectiveness

of LSH (Evdokimov et al., 2022; He et al., 2023; Iwaszko & Strzelecka, 2016; Karamimoghadam et al., 2024).

This chapter provides a comprehensive overview of LSH, examining the fundamental physical principles, process parameters, and resultant microstructural and mechanical modifications. Additionally, it compares LSH with conventional surface hardening methods, highlights current industrial applications, and discusses future trends and challenges in the field. In this context, the chapter aims to equip researchers, engineers, and practitioners with a deep understanding of LSH's potential to meet the increasing demands for high-performance, durable materials in cutting-edge industries such as the automotive, aerospace, energy, and biomedical sectors.

2. Historical Development and Significance of Surface Hardening

The concept of surface hardening has a long and rich history, deeply rooted in the early practices of metallurgy and blacksmithing. For centuries, craftsmen recognized the importance of selectively hardening the working edges of tools, weapons, and other implements to enhance their durability and wear resistance. Traditional methods, such as quenching, involved heating a metal part followed by rapid cooling in water or oil to induce a hardened surface layer. Although these early techniques lacked precise control, they laid the foundation for the modern surface hardening technologies that rely on scientific principles and controlled processing conditions (Anusha et al., 2020).

With the increasing demands for more reliable and durable components, various surface engineering techniques have been developed to enhance the performance of metallic materials. Among the earliest of these methods are carburizing and nitriding, both of which modify the surface composition of steel to improve its mechanical properties (Mittemeijer & Somers, 2015). Carburizing involves the diffusion of carbon into the surface at elevated temperatures, resulting in a hard and wear-resistant outer layer while maintaining a tough and ductile core (Selcuk et al., 2000). Similarly, nitriding introduces nitrogen into the surface to form hard nitrides, thereby improving fatigue strength and corrosion resistance (Fossati et al., 2011; Genel & Demirkol, 2000). Subsequently, more advanced thermal surface hardening methods such as induction and flame hardening were introduced. These techniques allow for rapid and localized heating of specific regions of a component, enabling precise control over the hardened areas with minimal distortion of the overall geometry (Aswad et al., 2021; Grönegress, 2013). Such surface modifications enable controlled and repeatable enhancements to improve the performance of metal components across various industries. Figure 1 illustrates the evolution and diversity of

surface hardening technologies over time, highlighting how high integration capability has become an increasingly critical requirement for manufacturing systems. Alongside these advancements, physical methods such as plasma nitriding have made significant progress, particularly by enabling modifications to surface chemistry and microstructure at relatively low processing temperatures. These techniques not only preserve dimensional stability but also allow for the effective treatment of a broader and more diverse range of materials (Aghajani & Behrangi, 2017).

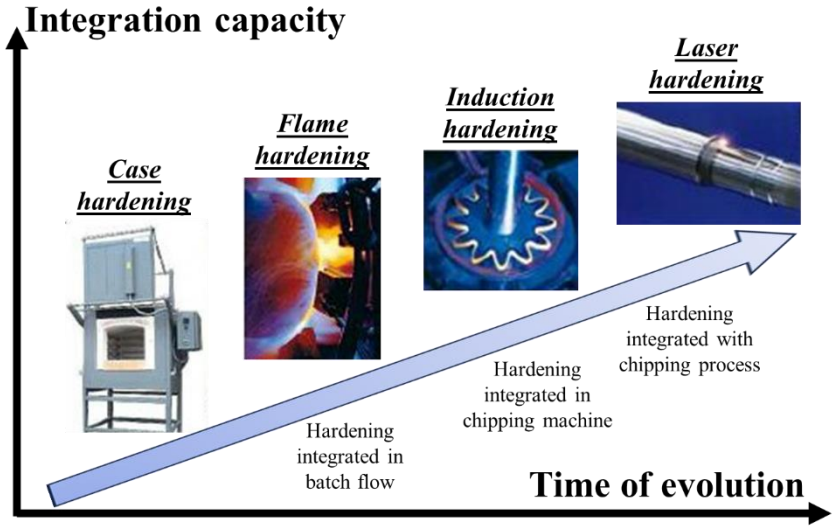

Figure 1. Evolution of surface hardening technologies (Roderburg et al., 2011)

The advent of laser-based technologies signified a major milestone in the development of surface hardening methods. This innovative approach combines the benefits of a highly concentrated energy source with exceptional process control and rapid thermal cycles, enabling the creation of hardened surface layers with minimal thermal influence on the substrate and almost no distortion. Such capabilities allow for precise manipulation of the surface treatment process, resulting in enhanced surface hardness through rapid heating and cooling without compromising the underlying material. As a result, LSH has established itself as a fundamental technique in current surface engineering practices (J. C. Ion, 2002; Kennedy et al., 2004). To further illustrate the principle and process of LSH, a schematic representation of the laser surface hardening procedure is provided in Figure 2.

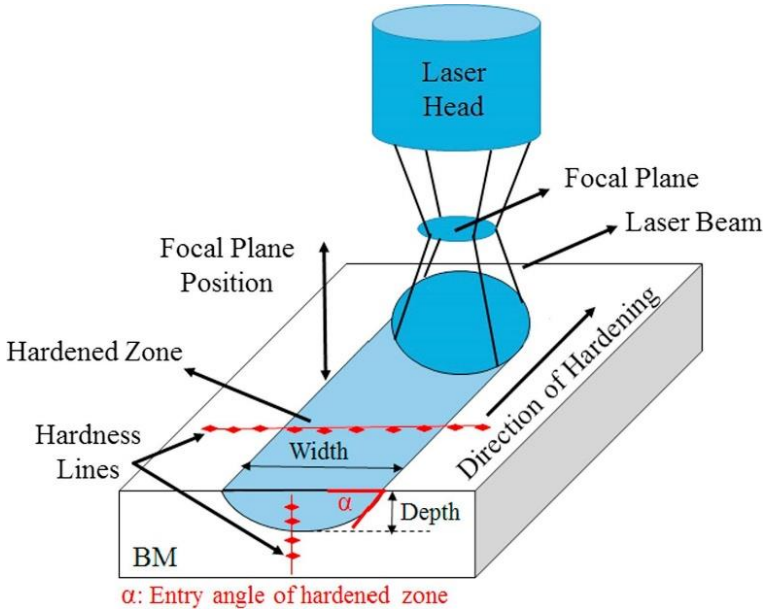

Figure 2. Schematic illustration of the LSH process (Khorram et al., 2019)

3. Fundamentals of Laser Surface Hardening

Laser surface hardening is a sophisticated surface engineering technique that utilizes the high energy density of laser beams to selectively heat the surface layer of metallic materials, inducing rapid thermal cycles that modify microstructure and enhance mechanical properties. Unlike traditional hardening methods, LSH offers exceptional precision, minimal distortion, and the ability to treat complex geometries. Understanding the fundamental interactions between the laser and material, the heat transfer dynamics, the types of lasers employed, and the control of process parameters is crucial for optimizing LSH performance and outcomes (Łach, 2024).

3.1. Laser–Material Interaction and Phase Transformations in LSH

In LSH, the fundamental process initiates with the direct interaction between the focused laser beam and the material's surface. When the laser photons strike the surface, they are absorbed, generating rapid and highly localized heating in a confined region. The efficiency of this absorption depends on multiple factors, including the laser wavelength, the optical properties of the material such as its reflectivity and absorptivity surface roughness, and the temperature of the surface at the time of irradiation. These parameters collectively influence how effectively the laser energy is converted into heat, which is critical for achieving the desired

thermal profile. Figure 3 shows the LSH mechanism, energy transfer, and microstructure.

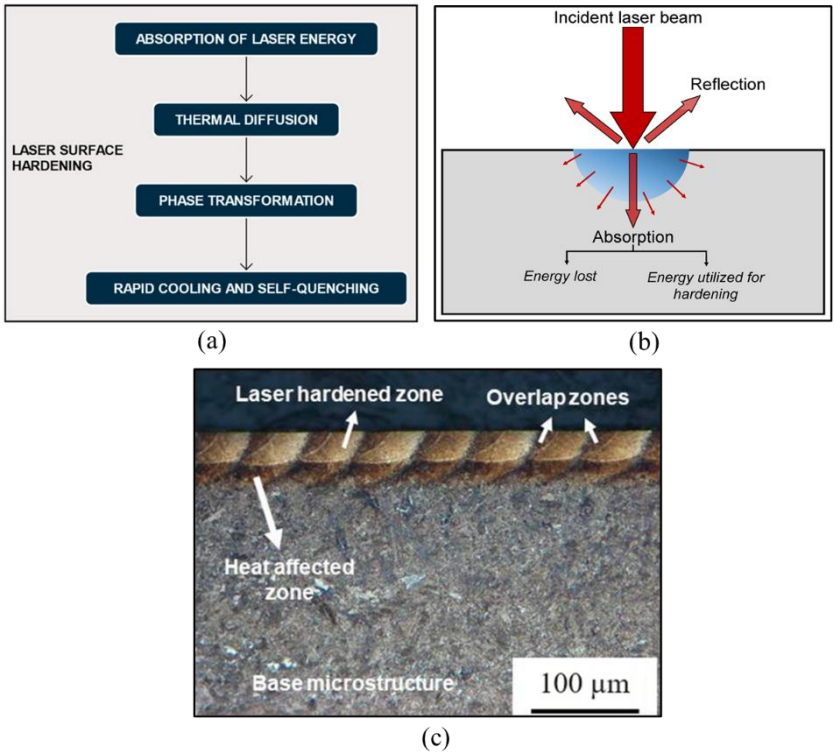

Figure 3. (a) LSH mechanism (Łach, 2024), (b) laser energy transfer during LSH (Maharjan et al., 2021), (c) microstructure after LSH (Maharjan et al., 2019)

The intense and localized heating caused by the laser rapidly raises the surface temperature beyond critical phase transformation thresholds, such as the austenitizing temperature in steels, thereby initiating the formation of new microstructures within the surface layer. As the laser beam scans over the surface and moves forward, the relatively cooler bulk substrate acts as a heat sink, quickly extracting heat from the heated zone. This results in a self-quenching effect of the treated surface layer. The rapid cooling rate prevents the formation of softer phases and instead favors the development of hard, metastable structures like martensite. These newly formed microstructures significantly enhance the surface hardness and contribute to improved wear resistance, which are primary goals of the LSH process. Achieving the optimal balance in the laser energy input is essential; it must be sufficient to induce the necessary phase transformations

while avoiding excessive heating that could lead to surface melting or other defects. Maintaining this balance ensures an effective hardening process that produces a defect-free, hardened layer with the desired mechanical properties (Barka et al., 2020; Lu et al., 2020; B. Wang, Pan, Liu, Lyu, et al., 2020).

3.2. Laser Types and Process Parameters in LSH

In LSH, common laser types are employed, each providing distinct advantages depending on the application, as illustrated in Figure 4.

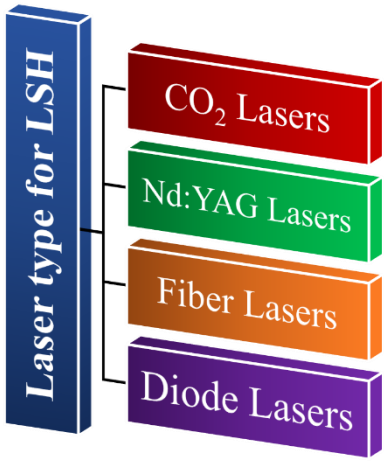

Figure 4. Common laser types used in LSH

The choice of laser, such as CO_2, Nd:YAG, fiber, or diode lasers, affects key factors like energy delivery, penetration depth, and process control. These differences enable precise tailoring of the hardening process to suit different materials and component geometries.

- CO_2 Lasers: Emit infrared radiation (around 10.6 μm wavelength), providing high power levels suitable for large-area hardening but with relatively lower beam quality.
- Nd:YAG Lasers: Operate at 1.064 μm, offering better beam quality and shorter wavelength, allowing for finer control and higher absorption in metals.
- Fiber Lasers: Known for their excellent beam quality, efficiency, and compactness, fiber lasers operate typically near 1 μm wavelength and are increasingly popular for industrial LSH applications.
- Diode Lasers: Provide lower power but high efficiency and can be combined in arrays for surface treatment.

Successful LSH depends on precise control of key parameters, including laser power, scanning speed, beam diameter, focal position, and shielding gas environment. These parameters influence the heat input, cooling rates, and thus the microstructure and hardness of the treated surface. For example, excessive power or slow scanning may cause surface melting or distortion, while insufficient energy results in inadequate hardening depth. Modern LSH systems integrate real-time monitoring and feedback mechanisms to optimize these parameters, ensuring consistent and defect-free treatments. Shielding gases such as argon or nitrogen are often used to prevent oxidation during processing (Łach, 2024).

4. Microstructural and Mechanical Modifications by LSH

LSH produces a defect-free hardened layer characterized by a fine, homogeneous microstructure, typically ranging from several hundred micrometers to over a millimeter in thickness, depending on processing parameters and material type. The process involves rapid localized heating above critical phase transformation temperatures, such as the austenitizing temperature in steels, which dissolves carbides and homogenizes the microstructure. This is immediately followed by rapid self-quenching facilitated by the cooler substrate, preventing the formation of equilibrium phases and promoting the development of hard, metastable microstructures like martensite. The resulting refined grain structure enhances hardness, toughness, and wear resistance. Additionally, LSH creates a narrow heat-affected zone, preserving the bulk material properties while minimizing surface roughness increases through precise process control. The rapid quenching also induces compressive residual stresses, which improve fatigue life by inhibiting crack initiation and propagation. Consequently, components treated with LSH exhibit substantially increased surface hardness often two to four times higher than untreated materials along with superior wear resistance and fatigue performance, making this technique especially valuable in demanding applications such as automotive gears and aerospace parts (Jegadheesan et al., 2023; J. Wang et al., 2024).

5. Industrial Applications of LSH

LSH has found widespread adoption across various industries due to its precision, efficiency, and ability to improve component performance without compromising bulk material properties. The versatility of LSH allows it to be applied to a range of materials and component geometries, enabling significant enhancements in wear resistance, fatigue strength, and service life. In Figure 5, the main industrial sectors benefiting from LSH are shown.

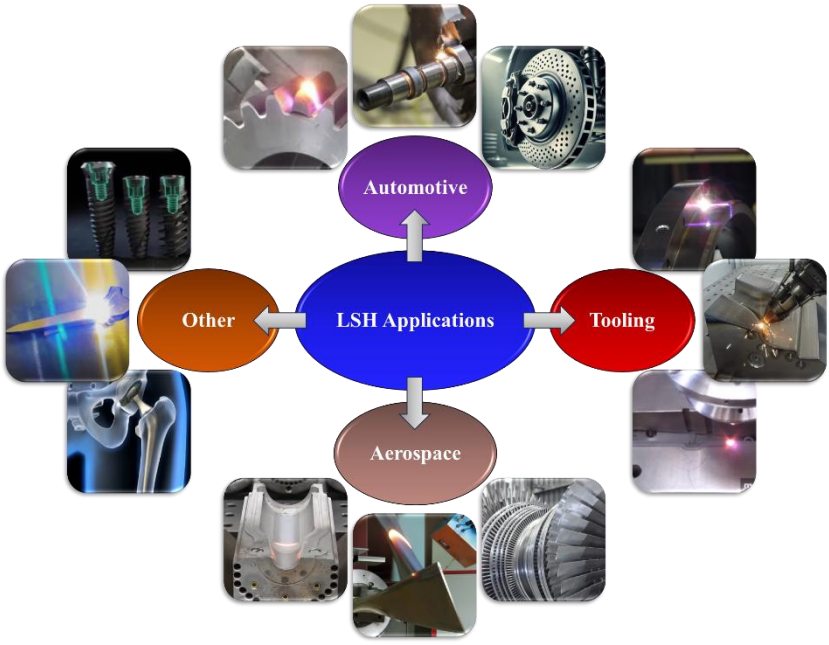

Figure 5. Main industries applying LSH

5.1. Automotive Components

The automotive industry heavily relies on components subjected to cyclic loads, friction, and wear, such as gears, camshafts, crankshafts, and valve components. LSH is widely employed to selectively harden these parts, improving their surface hardness and fatigue life while minimizing thermal distortion that could affect dimensional tolerances. The localized nature of LSH enables treatment of complex geometries and selective zones, optimizing performance without the need for extensive post-processing (Guarino et al., 2017; He et al., 2023; Karamimoghadam et al., 2024; Nemova, 2024).

5.2. Aerospace Applications

In aerospace and defense sectors, components often operate under extreme mechanical and environmental conditions, requiring materials with exceptional wear resistance, fatigue strength, and corrosion resistance. LSH is used to enhance critical parts such as turbine blades, landing gear components, and structural parts, where improved surface properties translate directly to increased safety and operational reliability. The rapid, precise processing of LSH also supports the stringent quality and repeatability demands of aerospace

manufacturing (Abbas et al., 2006; Adebiyi & Popoola, 2015; Kindrachuk et al., 2021).

5.3. Tooling Industry

Tools and dies used in metal forming, stamping, and extrusion processes experience severe wear and cyclic loading. LSH improves the surface hardness and wear resistance of these tools, significantly extending their service life and reducing downtime associated with tool replacement. Unlike conventional hardening methods that may cause distortion and dimensional changes, LSH ensures minimal thermal impact, preserving the precise geometry critical for tool performance. This results in cost savings and improved productivity in manufacturing environments (El-Batahgy et al., 2013; Han et al., 2014; J. Ion, 2005).

5.4. Other Applications

Although less common, LSH is gaining interest in biomedical applications, particularly for metallic implants such as orthopedic screws and dental implants. Surface hardening enhances wear resistance and fatigue life without compromising biocompatibility (Tan et al., 2024). Additionally, emerging applications in the energy sector, such as hardening of components in power generation and oil and gas industries, are also benefiting from the controlled, localized treatment that LSH provides (Kurnoskin et al., 2021; Lesyk et al., 2023). Ongoing research explores the integration of LSH with additive manufacturing processing to further expand its applicability (Łach, 2024).

6. Conclusion

Laser surface hardening has emerged as a powerful and versatile surface engineering technique that offers precise, rapid, and localized modification of material surfaces. By leveraging controlled laser–material interactions and self-quenching mechanisms, LSH significantly enhances surface hardness, wear resistance, and fatigue performance without compromising the bulk properties of components. Its ability to treat complex geometries with minimal thermal distortion makes it highly suitable for a wide range of industrial applications, including automotive, aerospace, tooling, and emerging biomedical fields.

Advancements in laser technology, process monitoring, and hybrid treatment approaches continue to expand the capabilities and effectiveness of LSH, addressing challenges related to process control, material compatibility, and treatment depth. Despite existing limitations, ongoing research and innovation

are driving wider adoption and integration of LSH within modern manufacturing frameworks.

Overall, LSH represents a critical evolution in surface hardening technologies, providing sustainable and efficient solutions to meet the increasing demands for high-performance materials in advanced engineering sectors. Continued interdisciplinary efforts will be essential to fully realize the potential of LSH and further enhance the durability, reliability, and functionality of engineered surfaces.

Acknowledgments

This research has been supported by Kafkas University Scientific Research Projects Coordination Unit. Project Number: 2025-FM-87 Year: 2025.

References

Abbas, G., Li, L., Ghazanfar, U. & Liu, Z. (2006). Effect of high power diode laser surface melting on wear resistance of magnesium alloys. *Wear*, *260*(1–2), 175–180.

Adebiyi, D. I. & Popoola, A. P. I. (2015). Mitigation of abrasive wear damage of Ti–6Al–4V by laser surface alloying. *Materials & Design*, *74*, 67–75.

Aghajani, H. & Behrangi, S. (2017). *Plasma nitriding of steels*. Springer.

Anusha, E., Kumar, A. & Shariff, S. M. (2020). A novel method of laser surface hardening treatment inducing different thermal processing condition for Thin-sectioned 100Cr6 steel. *Optics & Laser Technology*, *125*, 106061.

Aswad, M. F., Mohammed, A. J. & Faraj, S. R. (2021). Induction Surface Hardening: A review. *Journal of Physics: Conference Series*, *1973*(1). https://doi.org/10.1088/1742-6596/1973/1/012087

Barka, N., Sattarpanah Karganroudi, S., Fakir, R., Thibeault, P. & Feujofack Kemda, V. B. (2020). Effects of laser hardening process parameters on hardness profile of 4340 steel spline—an experimental approach. *Coatings*, *10*(4), 342.

Chen, Y., Zhao, X., Liu, P., Pan, R. & Ren, R. (2018). Influences of local laser quenching on wear performance of D1 wheel steel. *Wear*, *414*, 243–250.

Cui, Z., Shi, H., Wang, W. & Xu, B. (2015). Laser surface melting AZ31B magnesium alloy with liquid nitrogen-assisted cooling. *Trans. Nonferrous Met. Soc. China*, *25*(1446), 1453.

Duan, S., Ren, W., Lei, W. & Wang, Y. (2023). Study on the microstructure and properties of rail cladding layer after laser quenching. *Journal of Manufacturing Processes*, *108*, 180–193.

El-Batahgy, A.-M., Ramadan, R. A. & Moussa, A.-R. (2013). Laser surface hardening of tool steels—experimental and numerical analysis. *Journal of Surface Engineered Materials and Advanced Technology*, *3*(2), 146–153.

Evdokimov, A., Jasiewicz, F., Doynov, N., Ossenbrink, R. & Michailov, V. (2022). Simulation of surface heat treatment with inclined laser beam. *Journal of Manufacturing Processes*, *81*, 107–114.

Fossati, A., Galvanetto, E., Bacci, T. & Borgioli, F. (2011). Improvement of corrosion resistance of austenitic stainless steels by means of glow-discharge nitriding. In *Corrosion Reviews* (Vol. 29, Issues 5–6, pp. 209–221). https://doi.org/10.1515/CORRREV.2011.004

Genel, K. & Demirkol, M. (2000). Effect of ion nitriding on fatigue behaviour of AISI 4140 steel. In *Materials Science and Engineering* (Vol. 279). www.elsevier.com/locate/msea

Grönegress, H. W. (2013). *Flame hardening*. Springer Science & Business Media.

Guarino, S., Barletta, M. & Afilal, A. (2017). High Power Diode Laser (HPDL) surface hardening of low carbon steel: Fatigue life improvement analysis. *Journal of Manufacturing Processes*, *28*, 266–271.

Han, S. W., Joo, B. D. & Moon, Y. H. (2014). Selective surface hardening by laser melting of alloying powder. *Materials Research Innovations*, *18*(sup2), S2-902.

He, P., Ding, Y., Jiang, S., Zhang, H., Shen, T. & Wang, Y. (2023). Process parameters analysis of laser phase transformation hardening on the raceway surface of shield main bearing. *Photonics*, *10*(3), 287.

Ion, J. (2005). *Laser processing of engineering materials: principles, procedure and industrial application*. Elsevier.

Ion, J. C. (2002). Laser transformation hardening. *Surface Engineering*, *18*(1), 14–31.

Iwaszko, J. & Strzelecka, M. (2016). Effect of cw-CO2 laser surface treatment on structure and properties of AZ91 magnesium alloy. *Optics and Lasers in Engineering*, *81*, 63–69.

Jegadheesan, C., Somasundaram, P., Praveen Kumar, S., Vivek Anand, A. & Jeyaprakash, N. (2023). State of art: Review on laser surface hardening of alloy metals. *Materials Today: Proceedings*.

Karamimoghadam, M., Rezayat, M., Moradi, M., Mateo, A. & Casalino, G. (2024). Laser surface transformation hardening for automotive metals: Recent progress. *Metals*, *14*(3), 339.

Kennedy, E., Byrne, G. & Collins, D. N. (2004). A review of the use of high power diode lasers in surface hardening. *Journal of Materials Processing Technology*, *155*, 1855–1860.

Khorram, A., Davoodi Jamaloei, A., Jafari, A. & Moradi, M. (2019). Nd:YAG laser surface hardening of AISI 431 stainless steel; mechanical and metallurgical investigation. *Optics and Laser Technology*, *119*. https://doi.org/10.1016/j.optlastec.2019.105617

Kindrachuk, M., Dukhota, O., Tisov, O., Korbut, E., Yurchuk, A., Kharchenko, V. & Naumenko, N. (2021). Improving the wear resistance of heavy-duty elements in tribomechanical systems by a combined laser-thermochemical processing method. *Eastern-European Journal of Enterprise Technologies*, *3*(12), 111.

Kurnoskin, I. A., Krylova, S. E. & Plesovskikh, A. Y. (2021). Development of hardening technology for oil and gas pumping and compressor equipment using laser hardening. *Defect and Diffusion Forum*, *410*, 433–438.

Kusinski, J., Kac, S., Kopia, A., Radziszewska, A., Rozmus-Górnikowska, M., Major, B., Major, L., Marczak, J. & Lisiecki, A. (2012). Laser modification of the materials surface layer–a review paper. *Bulletin of the Polish Academy of Sciences: Technical Sciences*, *4*.

Łach, Ł. (2024). Recent advances in laser surface hardening: Techniques, modeling approaches, and industrial applications. *Crystals*, *14*(8), 726.

Lesyk, D., Hruska, M., Mordyuk, B., Kochmanski, P. & Powalka, B. (2023). Robot-Assisted 3D Laser Surface Hardening of Medium-Carbon Steel: Surface Roughness Parameters and Hardness. *International Conference "New Technologies, Development and Applications"*, 45–53.

Lu, Y., Meyer, H. & Radel, T. (2020). Multi-cycle phase transformation during laser hardening of AISI 4140. *Procedia CIRP*, *94*, 919–923.

Maharjan, N., Wu, N. & Zhou, W. (2021). Hardening efficiency and microstructural changes during laser surface hardening of 50crmo4 steel. *Metals*, *11*(12). https://doi.org/10.3390/met11122015

Maharjan, N., Zhou, W., Zhou, Y., Guan, Y. & Wu, N. (2019). Comparative study of laser surface hardening of 50CrMo4 steel using continuous-wave laser and pulsed lasers with ms, ns, ps and fs pulse duration. *Surface and Coatings Technology*, *366*, 311–320. https://doi.org/10.1016/j.surfcoat.2019.03.036

Mittemeijer, E. J. & Somers, M. A. J. (2015). *Thermochemical surface engineering of steels*. Woodhead Publishing.

Nemova, G. (2024). Brief review of recent developments in fiber lasers. *Applied Sciences*, *14*(6), 2323.

Roderburg, A., Klocke, F. & Koshy, P. (2011). Principles of technology evolutions for manufacturing process design. *Procedia Engineering*, *9*, 294–310. https://doi.org/10.1016/j.proeng.2011.03.120

Selcuk, B., Ipek, R., Karamis, M. B. & Kuzucu, V. (2000). An investigation on surface properties of treated low carbon and alloyed steels (boriding and carburizing). *Journal of Materials Processing Technology, 103(2), 310-317.*

Tan, C. Y., Wen, C. & Ang, H. Q. (2024). Influence of laser parameters on the microstructures and surface properties in laser surface modification of biomedical magnesium alloys. *Journal of Magnesium and Alloys*, *12*(1), 72–97.

Wagh, S. V, Bhatt, D. V, Menghani, J. V & Bhavikatti, S. S. (2020). Effects of laser hardening process parameters on hardness depth of Ck45 steel using Taguchi's optimization technique. *IOP Conference Series: Materials Science and Engineering*, *810*(1), 012027.

Wang, B., Barber, G. C., Wang, R. & Pan, Y. (2020). Comparison of wear performance of austempered and quench-tempered gray cast irons enhanced by laser hardening treatment. *Applied Sciences*, *10*(9), 3049.

Wang, B., Pan, Y., Liu, Y., Barber, G. C., Qiu, F. & Hu, M. (2020). Wear behavior of composite strengthened gray cast iron by austempering and laser hardening treatment. *Journal of Materials Research and Technology*, *9*(2), 2037–2043.

Wang, B., Pan, Y., Liu, Y., Lyu, N., Barber, G. C., Wang, R., Cui, W., Qiu, F. & Hu, M. (2020). Effects of quench-tempering and laser hardening treatment on wear resistance of gray cast iron. *Journal of Materials Research and Technology*, *9*(4), 8163–8171.

Wang, J., Xia, J., Liu, Z., Xu, L., Liu, J., Xiao, Y., Gao, J., Ru, H. & Jiao, J. (2024). A comprehensive review of metal laser hardening: mechanism, process, and applications. *The International Journal of Advanced Manufacturing Technology*, *134*(11), 5087–5115.

Chapter 3

A General Overview of Marine Sandwich Composite Materials

Mehmet ÖZER[1], Fatih BALIKOĞLU[2]

Abstract

The marine industry uses sandwich composite structures a lot because they can meet important needs like being lightweight, stiff, resistant to corrosion, and long-lasting in harsh environments. These structures have a lightweight core material sandwiched between two strong, thin face sheets. This makes them much stiffer when bent, while also making them lighter and allowing for more complex shapes. They can be used on a wide range of scales, from small boats to large ships, thanks to a few different manufacturing methods, such as hand lay-up, resin transfer molding, vacuum infusion, and prepreg processing. Along with geometric design, choosing the right materials is very important because both mechanical and environmental properties need to be considered. Sandwich composites have many benefits, such as better structural performance, less weight, resistance to corrosion, more design options, and less need for maintenance. However, their higher production costs are still a drawback compared to traditional materials like steel, aluminum, and wood. Glass, carbon, and aramid fiber-reinforced polymers are frequently used to make face sheets. Balsa wood, honeycomb structures, and polymer foams are frequently used to make cores. Polyester resins, vinyl ester, and epoxy are frequently used as matrix materials.

Keywords: Boat manufacturing, Core materials, Fiber-reinforced polymers, Sandwich composites.

1. INTRODUCTION

In the marine industry, criteria such as lightness, high rigidity, corrosion resistance, and fatigue performance are decisive factors in material selection. In line with these requirements, sandwich composite structures are widely used, particularly in boat hulls, deck panels, superstructure elements, and offshore platform components. Sandwich composites consist of a low-density but thick core material located between two thin, high-strength surface layers (skin) (Figure 1a). This

[1] Öğr. Gör. Dr. Balıkesir University, Bigadiç Vocational School, Department of Transportation Services Program, Balıkesir, Turkiye, Orcid: 0000-0002-6212-1217
[2] Doç. Dr. Balıkesir University, Faculty of Engineering, Department of Mechanical Engineering, Balıkesir, Turkiye, Orcid: 0000-0003-3836-5569

structure dramatically increases bending rigidity while minimizing weight (Figure 1b). Another advantage is their ability to manufacture complex geometry and forms essential for most boat components. Moreover, several manufacturing processes may be used, such as hand lay-up, resin transfer molding, vacuum infusion, or prepreg assembly, enabling preparation at various scales, ranging from small boats to large ships. (Palomba, Epasto, & Crupi, 2022)

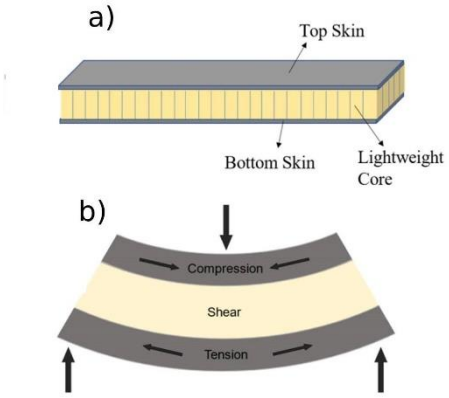

Figure 1. a) Sandwich composite structure; b) loading mechanics of sandwich panel (Singh, Sheikh, & Behera, 2024).

Today, numerous materials are available to produce sandwich composites. The list of materials has expanded significantly, particularly in recent years, with the introduction of fiber-reinforced polymers and cellular foam. Therefore, in the design of sandwich structures, material selection is as important as the geometric dimensioning process. The wide variety of available materials can seem complex, but the properties that enable the use of sandwich composite materials in marine environments must be prioritized. In specific applications, weak material properties are improved by refinements in geometric dimensioning: for example, sandwich structures exhibit less rigidity than metals, but a usable rigidity value can be achieved by increasing the core thickness.

In material selection, not only mechanical performance but also environmental resistance (UV, humidity, temperature, etc.), surface quality, production method, cost, wear resistance, etc. parameters should be considered. The basic properties required for the face sheets are high flexural rigidity, high tensile and compressive strength, surface quality, impact resistance, environmental resistance, and wear resistance. On the other hand, properties such as low density, high shear strength and rigidity, high compressive rigidity, sound and heat insulation are desired from the core material (Calabrese, Di Bella, & Fiore, 2016).

The reasons for the preference of sandwich composites in marine construction applications can be listed as follows.

- Thanks to its high bending strength and rigidity, it provides resistance against bending loads to which the hull beam is subjected in sagging and collapse situations (Zenkert, 1995).
- It has high impact resistance and is resistant to underwater shock loads (Sutherland, 2018a, 2018b, 2018c).
- It saves weight; it contributes to increased cargo capacity, fuel savings, higher acceleration and stability of the ship (Crupi, Epasto, & Guglielmino, 2013).
- It is resistant to corrosion (Alexandra Kootsookos & Burchill, 2004; Alex Kootsookos & Mouritz, 2004).
- It provides design and manufacturing flexibility (Karlsson & TomasÅström, 1997).
- Maintenance costs are low (Russell, 2005).
- It enables the production of complex and smooth hydrodynamic surfaces (Mazumdar, 2001).
- It has critical properties for military applications: low thermal, acoustic, magnetic and electromagnetic signatures (Mouritz, Gellert, Burchill, & Challis, 2001).

The advantages of sandwich structures in boat building are schematically summarized in Figure 2.

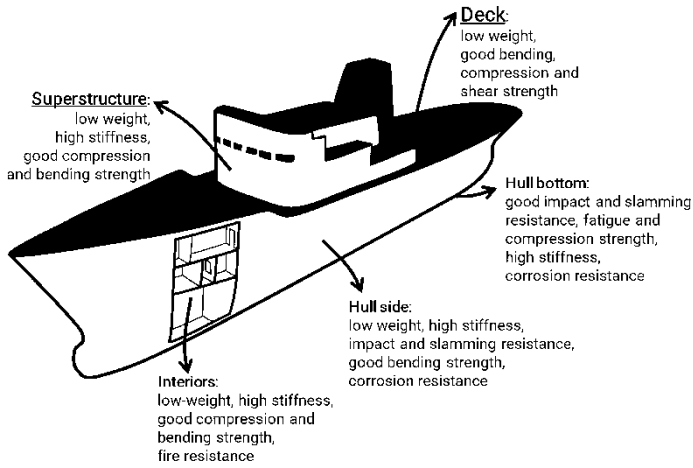

Figure 2. Benefits of sandwich structure applications in different areas of the boat (Palomba, Epasto, & Crupi, 2022).

A major disadvantage of sandwich composites is their higher production costs compared to traditional materials (steel, aluminum, and wood) because their production is labor-intensive. In marine sandwich composite structures, glass (Figure

3a), carbon (Figure 3b), aramid (Figure 3c) fiber-reinforced polymer matrix layers and polymer foams (specifically polystyrene (Figure 3d) or PVC foam (Figure 3e), balsa wood (Figure 3f), and honeycomb (Figure 3g) core materials are used. Epoxy, vinyl ester, and polyester resins are the three most common matrix materials for composite marine structures (Calabrese et al., 2016; Di Bella, Calabrese, & Borsellino, 2012; Kolat, Neşer, & Özes, 2007; Mitra, 2010; Mouritz et al., 2001).

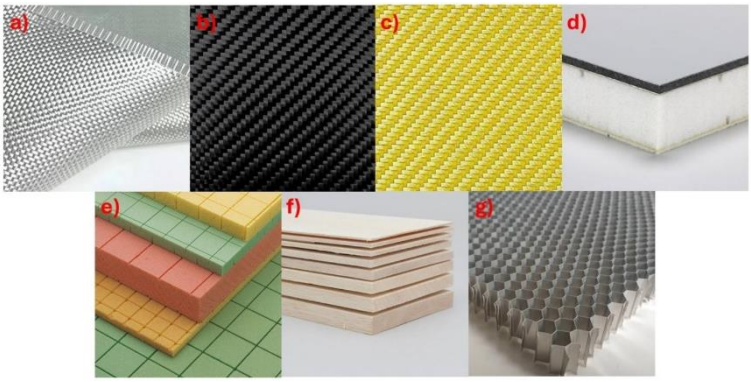

Figure 3. Core materials for marine composite materials. a) glass fiber, b) carbon fiber, c) aramid fiber, d) polystyrene foam, e) PVC foam, f) balsa wood, g) honeycomb.

2. REINFORCEMENT MATERIALS

Carbon and glass are two of the most used fiber types for marine applications (Figure 4, 5). Glass fibers are generally preferred in recreational boats due to their low cost and good chemical resistance, while carbon fibers are preferred in high-performance marine vessels (military corvettes, patrol boats, and racing yachts) where high strength and rigidity are required. The most common aramid fiber is Kevlar®, developed by DuPont.

Reinforcement material is the most effective element determining the mechanical properties of laminate composites. Therefore, when selecting a suitable fiber material for marine applications, resistance to environmental degradation should be considered. Degradation due to moisture varies among the available fibers. Although carbon fibers are susceptible to chemical attacks, they are resistant to seawater. Glass fiber, on the other hand, shows a decrease in strength values when exposed to seawater (Alex Kootsookos & Mouritz, 2004). Kevlar® 49 has higher moisture absorption than other reinforcements, although Kevlar® 149 has about two-thirds less moisture absorption than Kevlar® 49. In practice, the moisture absorption of fibers is reduced by resin matrix impregnation and external coating applications (gelcoat).

Fibers are produced as textile products in different forms so that they can be applied to production methods. The boat industry could not fully benefit from the directional anisotropic properties of glass fiber until unidirectional and woven fabric reinforcements were introduced to the market. In the early years, mat and chopped glass fiber reinforcements with isotropic properties were used in boat building. With the use of unidirectional fibers, the necessary stiffness values were provided in longitudinal strength elements such as hull beams or along the centerlines of the hull. With stitched bidirectional fibers with ±45 orientations, the shear strength of boat hulls increased and their resistance to torsional loads was improved. Today, fibers with various textile architectures; woven, stitched, unidirectional, and mat (non-woven) etc. reinforcement elements are used in the marine construction sector (Greene, 1997; Pemberton, Summerscales, & Graham-Jones, 2018).

Comparative properties of the most common reinforcement elements used in marine composite applications are given in Table 1. From 1997 to 2024, fiberglass maintained its superiority in terms of usage in boat manufacturing. Carbon fiber and Kevlar are regarded as the most widespread reinforcing materials after glass fiber. Hybrid fibers are used in boat construction. The proportion of use for the hull and deck exhibits minimal variation when considered in total.

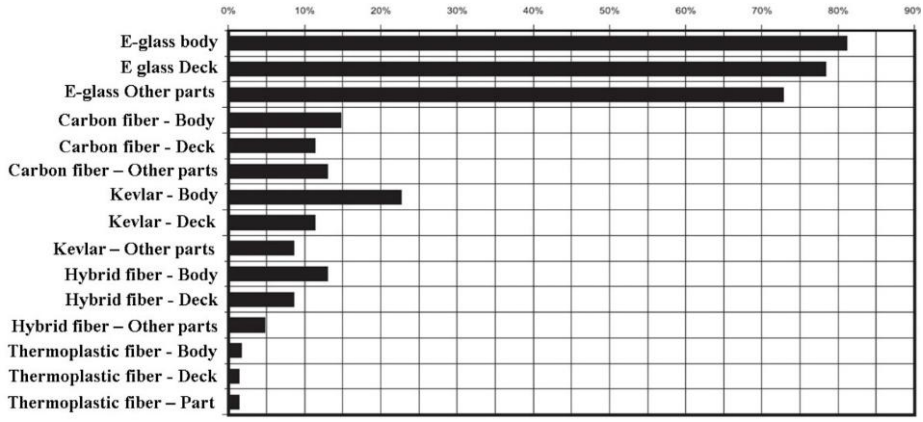

Figure 4. Use of reinforcement elements in marine composite materials (%) (Greene, 1997).

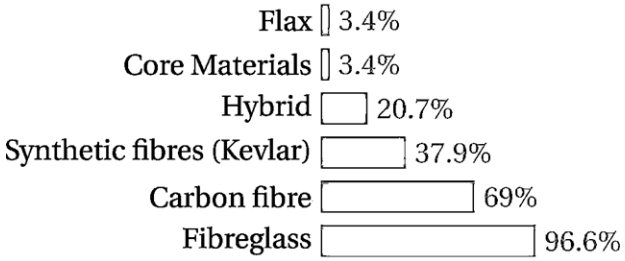

Figure 5. Survey results on EU shipyards about reinforcement materials (Dolz, Martinez, Sá, Silva, & Jurado, 2024).

Table 1. Comparison of the most common reinforcement elements used in marine applications.

Reinforcement Elements		
Glass Fiber (GFRP)	**Carbon Fiber (CFRP)**	**Aramid Fiber (Kevlar)**
Most-used composite.	High modulus of elasticity	High impact resistance
Cost-effective.	Low density	Difficult to machine
High corrosion resistance.	High cost	
Moderate mechanical properties.	High performance applications.	

3. CORE MATERIALS

Natural materials like balsa wood have long been preferred in sandwich structures due to their lightness and sustainability (Figure 6) (Castro, Silva, Devezas, Silva, & Gil, 2010; Gil, 2009; Reis & Silva, 2009). Balsa wood, with its honeycomb-like cell structure, has higher shear properties compared to PVC foam and other core materials (Cremonini, Negro, Properzi, & Zanuttini, 2008). Sandwich composites with balsa cores have been used, for example, in the advanced enclosed radar mast (AEM/S) cladding on the USS Arthur W. Radford destroyer and in many other marine applications (Di Bella et al., 2012; Ulven & Vaidya, 2006). Although balsa wood has excellent mechanical properties, polymer foams have been developed and introduced to the market as complementary options in the design of sandwich structures. PVC foams are the most preferred core material in the small and medium-sized boat and yacht manufacturing sector. Compared to balsa wood, these materials have superior properties such as low density, low moisture absorption capacity, and impact damage tolerance. These polymers are cellular materials classified in the open and closed-cell foam categories. In open-cell foams, the cells are interconnected, and seawater can penetrate throughout the thickness of the foam. For these reasons, closed-cell foams are preferred as core materials in marine sandwich

structures. The closed-cell structure helps achieve higher compressive strength and rigidity compared to open-cell foams. The gas trapped in the foam cells provides back pressure, which helps improve the compressive and impact properties of these materials. Chemically, PVC foams are classified as linear and cross-linked. Linear foams have lower static strength values but higher performance under impact load compared to cross-linked foams. Cross-linked PVC foams are more frequently used. In addition to the examples given, there are also core structures such as polystyrene foam, polyester nonwoven filler, wood plywood, phenolic and polypropylene honeycomb. The sensitivity of the core material to moisture is an important consideration for structural applications exposed to seawater. Moisture absorption affects the mechanical, electrical, and thermal insulation properties of the sandwich structure. Large dimensional changes and even damage resulting in swelling, bulging, and delamination can occur due to moisture absorption. Therefore, plywood and honeycomb structures have not found widespread application due to their high moisture absorption capacity. Polystyrene foam, on the other hand, has limited its use due to its low mechanical properties and its reaction with polyester resin. Polyester nonwoven fillers are used to increase the thickness in laminate boat decks (Greene, 1997; Pemberton et al., 2018). Table 2 shows a comparative analysis of the properties of some of the most used core materials in marine applications.

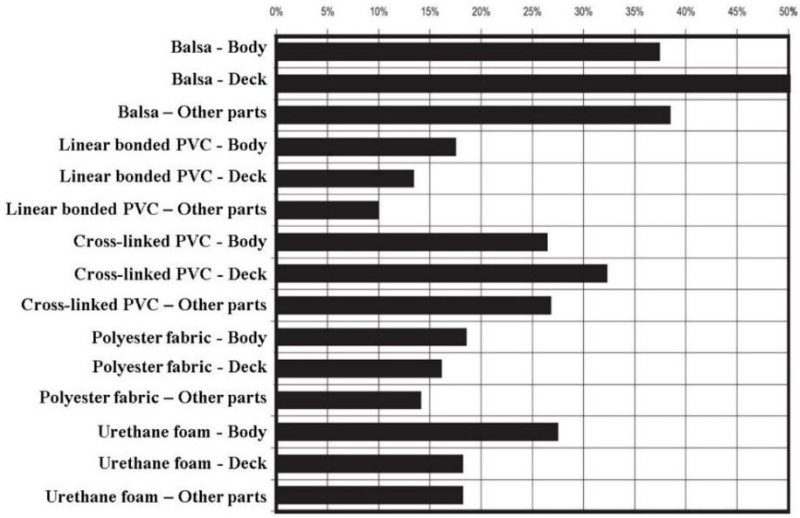

Figure 6. Core material usage in marine composite materials (%) (Greene, 1997).

Table 2. Comparison of the most common core materials used in marine applications.

Core Materials			
PVC	**PET**	**Balsa Wood**	**Honeycomb**
Closed cell structure	Recyclable	High compressive strength	High rigidity/weight ratio
Low water absorption	Better thermal stability	Natural material	Aluminum or Nomex
Medium density	Environmental sustainability	Risk of water damage	Risk of water penetration

4. RESINS

Polyester resins have lower mechanical properties and a higher risk of moisture absorption compared to their vinyl ester and epoxy competitors. There are two types of polyester resins: orthophthalic and isophthalic. Due to their low cost, polyester resins are widely used in less critical applications such as the construction of small pleasure boats (Figure 7,8). In such boats, gelcoat or barrier applications are relied upon to act as a protective barrier between the composite structure and seawater against moisture absorption. Isophthalic polyester resins, which exhibit greater resistance to water absorption, are used in these outer coatings.

Vinyl esters typically fall between epoxy and polyester resins in terms of mechanical performance and cost. Due to their low moisture absorption values, vinyl esters are widely used in boat building and other marine structures. In these resins, the catalyst and resin mixing ratios can vary depending on environmental conditions such as heat and humidity. In addition, their high resistance to chemicals and environmental degradation compared to polyesters makes these resins suitable for marine applications.

Polyester and vinyl ester resins contain styrene, which causes the release of harmful volatile organic gases (VOCs) during curing. Ventilation systems are essential in factories to protect workers from styrene, solvent, and catalyst vapors, which pose potential health risks. Even these measures may not prevent the inhalation of styrene vapor in the factory area. Therefore, resins with low styrene content are preferred.

Epoxy resins, on the other hand, have higher mechanical properties and better resistance to environmental degradation than vinyl ester or polyester resins. In epoxy applications, the hardener and resin mixing ratios are constant. While polyester and vinyl ester resins show shrinkage between 7% and 10% after curing, epoxy resins have shrinkage values lower than 2%. This ensures that the products coming out of

the mold have smooth surfaces (Chalmers, 1994; Greene, 1997; Hoge & Leach, 2016; Marsh, 2007; Pemberton et al., 2018).

From 1997 to 2024, the use of polyester and vinyl ester in the maritime industry remained constant, but the application of epoxy showed an increase. It is essential to note that whereas most general-purpose epoxies provide strong adhesion and surface protection, they frequently suffer from problems such as swelling, hydrolysis, and UV-induced delamination when exposed to long marine conditions. Marine-grade epoxy formulas improve water absorption rates, use specific crosslinkers to prevent salt or moisture degradation, and show a durable character that endures hull bending and vibration without losing adhesion. The acceptance and rising popularity of epoxy resin in maritime applications by engineers and shipbuilders may be attributed to its adherence to a strictly defined set of qualities and requirements.

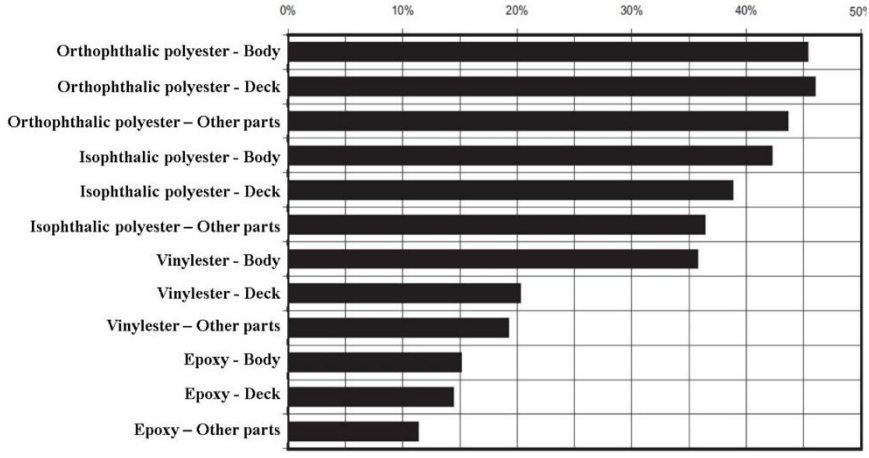

Figure 7. Resin usage in marine composite materials (%) (Greene, 1997).

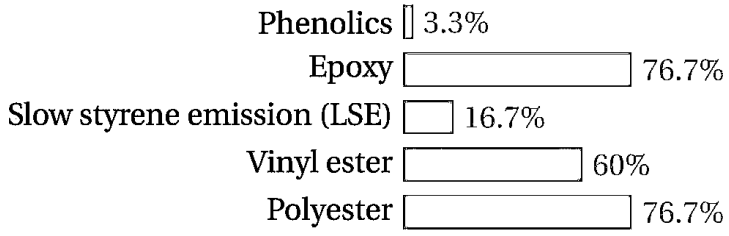

Figure 8. Survey results on EU shipyards about resin materials (Dolz, Martinez, Sá, Silva, & Jurado, 2024).

5. COMPOSITE BOAT PRODUCTION METHODS

According to a review of the literature, the most often used techniques for producing maritime composites are Hand Lay-Up, Vacuum Infusion, and Resin Transfer Molding (RTM), according to a review of the literature (Figure 9). However, the choice of which production method to use varies depending on the type of marine vessel and the location of the part to be produced on the vessel. Table 3 details the differences between these production methods. Furthermore, marine vessels made from composite structures are expected to withstand certain stresses during use. These challenging conditions include wave-induced bending, local impact loads, fatigue, hydrostatic pressure, and thermal cycling mechanisms. When subjected to these challenging conditions, the main damage mechanisms naturally occur. These damage mechanisms are defined as delamination, core crushing, surface buckling, and water penetration.

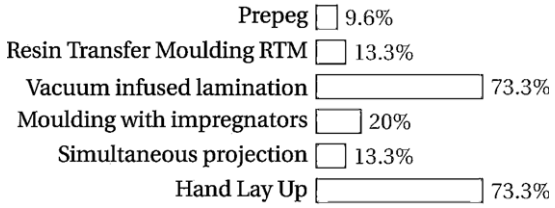

Figure 9. Survey results on EU shipyards about manufacturing processes (Dolz, Martinez, Sá, Silva, & Jurado, 2024).

Table 3. Types of marine composite production.

Production Method		
Hand Lay-Up	**Vacuum Infusion**	**RTM**
Low cost	High resin control	High quality
Small production volume	Lower void ratio	Controlled curing
Quality dependent on workmanship	Common in large boat hulls	High cost

Marine sandwich composite materials are advanced engineering solutions that meet the lightness, strength, and performance requirements of modern boat and shipbuilding. Optimized design with the right core and surface combination delivers superior results in terms of both economy and performance. In the future, the attainment of sustainability and the use of additive manufacturing methods in marine vessels are anticipated to lead to a variety of these structures and further expansion of their application areas.

REFERENCES

Calabrese, L., Di Bella, G., & Fiore, V. (2016). Manufacture of marine composite sandwich structures *Marine Applications of Advanced Fibre-Reinforced Composites* (pp. 57-78): Elsevier.

Castro, O., Silva, J. M., Devezas, T., Silva, A., & Gil, L. (2010). Cork agglomerates as an ideal core material in lightweight structures. *Materials & Design, 31*(1), 425-432.

Chalmers, D. (1994). The potential for the use of composite materials in marine structures. *Marine Structures, 7*(2-5), 441-456.

Cremonini, C., Negro, F., Properzi, M., & Zanuttini, R. (2008). *Wood-based composites in marine craft: The state of the art in Italy.* Paper presented at the COST Action E49 International Workshop in Slovenia on Lightweight Wood-Based Composites-Production, Properties and Usage. Bled.

Crupi, V., Epasto, G., & Guglielmino, E. (2013). Comparison of aluminium sandwiches for lightweight ship structures: Honeycomb vs. foam. *Marine Structures, 30*, 74-96.

Di Bella, G., Calabrese, L., & Borsellino, C. (2012). Mechanical characterisation of a glass/polyester sandwich structure for marine applications. *Materials & Design, 42*, 486-494.

Dolz, M., Martinez, X., Sá, D., Silva, J., & Jurado, A. (2024). Composite materials, technologies and manufacturing: Current scenario of European Union shipyards. Ships and Offshore Structures, 19(8), 1157-1172.

Gil, L. (2009). Cork composites: a review. *Materials, 2*(3), 776-789.

Greene, E. (1997). Design guide for marine applications of composites.

Hoge, J., & Leach, C. (2016). Epoxy resin infused boat hulls. *Reinforced Plastics, 60*(4), 221-223.

Karlsson, K. F., & TomasÅström, B. (1997). Manufacturing and applications of structural sandwich components. *Composites Part A: Applied Science and Manufacturing, 28*(2), 97-111.

Kolat, K., Neşer, G., & Özes, Ç. (2007). The effect of sea water exposure on the interfacial fracture of some sandwich systems in marine use. *Composite Structures, 78*(1), 11-17.

Kootsookos, A., & Burchill, P. (2004). The effect of the degree of cure on the corrosion resistance of vinyl ester/glass fibre composites. *Composites Part A: Applied Science and Manufacturing, 35*(4), 501-508.

Kootsookos, A., & Mouritz, A. P. (2004). Seawater durability of glass-and carbon-polymer composites. *Composites Science and Technology, 64*(10-11), 1503-1511.

Marsh, G. (2007). Vinyl ester–the midway boat building resin. *Reinforced Plastics, 51*(8), 20-23.

Mazumdar, S. (2001). *Composites manufacturing: materials, product, and process engineering*: CrC press.

Mitra, N. (2010). A methodology for improving shear performance of marine grade sandwich composites: Sandwich composite panel with shear key. *Composite Structures, 92*(5), 1065-1072.

Mouritz, A., Gellert, E., Burchill, P., & Challis, K. (2001). Review of advanced composite structures for naval ships and submarines. *Composite Structures, 53*(1), 21-42.

Palomba, G., Epasto, G., & Crupi, V. (2022). Lightweight sandwich structures for marine applications: a review. Mechanics of Advanced Materials and Structures, 29(26), 4839-4864.

Pemberton, R., Summerscales, J., & Graham-Jones, J. (2018). *Marine composites: design and performance*: Woodhead Publishing.

Reis, L., & Silva, A. (2009). Mechanical behavior of sandwich structures using natural cork agglomerates as core materials. *Journal of Sandwich Structures & Materials, 11*(6), 487-500.

Russell, C. (2005). Composites: long-term viability and benefits. *Reinforced Plastics, 49*(9), 36-42.

Sutherland, L. (2018a). A review of impact testing on marine composite materials: Part I–Marine impacts on marine composites. *Composite Structures, 188*, 197-208.

Sutherland, L. (2018b). A review of impact testing on marine composite materials: Part II–Impact event and material parameters. *Composite Structures, 188*, 503-511.

Sutherland, L. (2018c). A review of impact testing on marine composite materials: Part III-Damage tolerance and durability. *Composite Structures, 188*, 512-518.

Singh, P., Sheikh, J., & Behera, B. K. (2024). Metal-faced sandwich composite panels: A review. Thin-Walled Structures, 195, 111376.

Ulven, C., & Vaidya, U. (2006). Post-fire low velocity impact response of marine grade sandwich composites. *Composites Part A: Applied Science and Manufacturing, 37*(7), 997-1004.

Zenkert, D. (1995). An introduction to sandwich structures.

Chapter 4

Hydrochar-Derived Activated Carbons from Biomass via Hydrothermal Carbonization: Process Parameters and Optimization

Merve Nazlı BORAND[1]

Abstract

Hydrothermal carbonization (HTC) has established itself as an important thermochemical technology for converting wet lignocellulosic biomass into hydrochar, an intermediate for producing high-performance activated carbons. Unlike conventional pyrolysis or torrefaction, HTC operates under subcritical aqueous conditions (180-260 °C, 2-10 MPa), thereby eliminating the energy-intensive drying step and offering significant cost savings and sustainability benefits. The present chapter undertakes an integrated review of the entire HTC-to-activated-carbon production chain. The reaction chemistry of HTC is first investigated, highlighting the unique conversion mechanisms of cellulose, hemicellulose, and lignin via hydrolysis, dehydration, decarboxylation, condensation, and aromatization. A detailed analysis of the most significant operational parameters, temperature, residence time, liquid-to-biomass ratio, biomass composition, and pH.

Three chemical activation approaches, employing KOH, H_3PO_4, and $ZnCl_2$, are compared with the physical activation route. The former approach, employing KOH, consistently yields the highest BET surface area (>1000 m^2/g) via a redox reaction mechanism at 700-800 °C. H_3PO_4 activation also produces mesoporous carbons, albeit at lower temperatures (350-500 °C), whereas $ZnCl_2$ activation produces micro-mesoporous carbons via a molten salt templating mechanism. The most significant application areas, such as water treatment, CO2 capture, heavy metal removal, and electrochemical energy storage, are also discussed in relation to the established relationships between structure and property.

Keywords: Hydrothermal carbonization, activated carbon, process parameters, optimization, adsorption

[1] Assistant Prof. Dr., Yalova University, ORCID: 0000-0001-9068-065X

1. Introduction

The increasing sense of urgency regarding climate change, resource depletion, and the need for a circular economy has led to a global shift in materials science, moving from fossil-based carbon materials to renewable, waste-based carbon materials [1]. Carbon-based porous materials, particularly activated carbon, play a central role in this shift, as they underpin several critical technologies in modern society, including water and air purification, gas separation, heterogeneous catalysis, and electrochemical energy storage [2–4]. However, it is also clear that the dominant method of activated carbon production relies on fossil carbon sources, such as coal, lignite, and petroleum coke, which account for many global feedstocks [5,6]. Thus, the discovery of abundant, renewable, and cost-effective feedstocks for producing high-performance activated carbon remains a key challenge in the field [6].

Lignocellulosic biomass and agro-residues are, in fact, the most promising renewable feedstocks for the sustainable production of activated carbon. These biomass materials, which include rice husk, coconut shells, wood chips, sugarcane bagasse, corn cobs, tea waste, nut shells, etc., are carbon-rich, widely available, and essentially free or even cost-negative [7–14]. Moreover, the heterogeneity of these materials, in terms of variations in the proportion of cellulose, hemicellulose, and lignin, also offers a significant opportunity, as understanding the role of these components in determining the quality of the carbon precursor can help in the development of a robust process that can handle a variety of waste materials, thus facilitating region-specific solutions without the need for a particular feedstock [15,16].

Among thermochemical conversion technologies for wet lignocellulosic biomass, including pyrolysis, torrefaction, and gasification, hydrothermal carbonization (HTC) has arguably become the most promising process [17,18]. HTC involves the carbonization of wet lignocellulosic biomass in water at sub-critical temperature conditions (ranging between 180 and 250°C) and autogenous pressure (ranging between 2 and 10 MPa), thus circumventing the need for a costly pre-drying process, which is a major drawback for the economic viability of the conventional thermal conversion technologies [19–21]. As a result, a series of interrelated chemical reactions, which include hydrolysis, dehydration, decarboxylation, condensation, and subsequent aromatization, occur, thereby producing hydrochar, a carbon-rich, chemically reactive material that contains many active sites, which include a variety of oxygen functional groups such as carboxyl, hydroxyl, and carbonyl, on its surface [22].

Hydrochar is activated to activated carbon using chemical or physical activation methods at high temperatures (500-900 °C) [5,23]. Among chemical

activation methods using KOH, H_3PO_4, $ZnCl_2$, etc., KOH-based activation has been found to produce activated carbons with the highest surface areas, often exceeding 1000 m^2/g and reaching 3000 m^2/g under optimized activation conditions, and to feature well-developed microporous structures for adsorption and energy storage [24–29]. Nevertheless, the properties of the activated carbon produced are not solely a function of the activation step; rather, they are a cumulative result of the entire activation process, starting from the raw material selection and HTC process conditions (temperature, residence time, S:L ratio) to the type of activation chemical, impregnation ratio, and activation temperature. Such a multi-variable and multi-stage approach to activated carbon synthesis may appear complex; however, it also holds great promise for optimizing multiple interacting parameters to produce activated carbons with properties that may not be achievable through traditional one-variable optimization methods.

In this chapter, an integrated review of the HTC-to-activated-carbon production chain is provided, with particular focus on how HTC process conditions influence precursor characteristics, which in turn affect activation performance. The chapter begins with the chemistry and mechanisms of the HTC process, followed by the major HTC process conditions: temperature, residence time, solid-to-liquid ratio, feedstock, and pH. Subsequently, the chapter addresses the comparison of the three major chemical activation methods using KOH, H_3PO_4, and $ZnCl_2$, in addition to the physical activation process. The chapter concludes with the major application fields of HTC-based activated carbons and the challenges that remain to be overcome in implementing the HTC process.

2. HTC Fundamentals

HTC is a thermochemical conversion process in which wet biomass is treated in liquid water at subcritical temperatures between 180 and 260 °C under autogenously generated pressures of 2 to 10 MPa for residence times between 0.5 and 24 h. The key to HTC is the use of pressurized liquid water as the reaction medium and heat-transfer agent. This approach has several important advantages compared to other thermochemical processes. It avoids the need for energy-intensive biomass drying, exploits the unique physicochemical properties of hot, compressed water as a catalyst and solvent, and produces a carbon-rich solid product (hydrochar), a nutrient-rich liquid product, and a small amount of gases, mostly CO_2 [30,31]. In addition to the general advantages of HTC in energy efficiency and sustainability, a deep understanding of the process's fundamental chemistry and reaction pathways is essential for the rational design of the hydrochar precursor composition for subsequent use in the synthesis of activated carbon.

2.1 Reaction Chemistry and Mechanisms

During the complex and simultaneous set of reactions that make up the process, the three main biopolymeric constituents of plant biomass, cellulose, hemicellulose, and lignin, are decomposed into soluble compounds and finally into the aromatic and oxygen-containing carbon matrix of hydrochar [32]. The reaction medium has a significant impact on the course and result of the reaction. As temperature increases, the ion product of water rises, thereby increasing its ability to act as a catalyst for acid- and base-catalyzed reactions. The organic acids formed during biomass decomposition also have a pH-reducing effect and act as autocatalysts that accelerate the hydrolysis of glycosidic bonds in the polysaccharide fractions [9,33].

2.1.1 Cellulose transformation

Cellulose, the most abundant biopolymer on Earth, constitutes 30-50 wt% of lignocellulosic biomass. Cellulose consists of linear D-glucopyranose molecules connected by β-(1→4) glycosidic bonds [34,35]. Its high level of crystallinity, resulting from a high density of hydrogen bonds between and within molecules, makes cellulose resistant to thermal and chemical treatments under ambient conditions. Hydrothermal treatment, involving hot compressed water, breaks hydrogen bonds and enters the cellulosic matrix. This process converts crystalline cellulose into its amorphous form, which is more reactive [13]. Hydrolysis of this form yields glucose monomers and oligomers, which are then dehydrated to 5-hydroxymethylfurfural (5-HMF), the main intermediate formed during the hydrothermal treatment of hexose-containing materials. This intermediate then polymerizes and condenses into colloidal carbon particles and, eventually, into secondary hydrochar, which appears as carbon microspheres visible under electron microscopy [36]. Cellulose begins to show signs of reactivity at about 200 °C; below this temperature, cellulose conversion is limited [4,15,16].

2.1.2 Hemicellulose transformation

Hemicellulose, which constitutes 15 wt% to 35 wt% of lignocellulosic biomass, is a branched heteropolysaccharide composed of pentose (C5) and hexose (C6) sugars linked by β(1,4) glycosidic bonds [35]. Its branched and amorphous structure makes it the most hydrolyzable of the three components. In hydrothermal carbonization (HTC), under typical conditions, hemicellulose is almost completely hydrolyzed, yielding monosaccharide products that dehydrate to furfural and 5-HMF. Furfural has proven to be a significant intermediate in the HTC of hemicellulose. The ease of hemicellulose hydrolysis at relatively low HTC temperatures makes its content a critical factor in determining hydrochar

yield and the density of oxygen-containing functional groups under mild HTC conditions [15,16].

2.1.3 Lignin transformation

Lignin, the third component of lignocellulosic biomass, constitutes 15 wt% to 30 wt% of lignocellulosic biomasses. Lignin is a complex, randomly cross-linked aromatic polymer composed of phenylpropanoid units linked by C-O-C and C-C bonds [17]. The conversion mechanism of lignin under hydrothermal carbonization differs significantly from that of the other two components. The initial step involves the dealkylation and hydrolysis of C-O-C bonds in dissolved lignin fragments, yielding methoxyphenolics. Subsequent conversion to phenolic compounds occurs through competitive demethoxylation, alkylation, and condensation reactions [4,15]. The relative ease of breaking C-O-C bonds compared to C-C bonds controls the conversion rates. The phenolic compounds are converted into a new polymer via repolymerization through cross-linking reactions, resulting in a primary hydrochar. This process occurs almost exclusively through a solid-to-solid conversion mechanism. Primary hydrochar has a distinct structure and morphology compared to the microsphere-dominated secondary hydrochar resulting from cellulose and hemicellulose. Lignin, being more resistant to hydrothermal carbonization than the other two components, positively affects hydrochar yield and HHV [17].

3. Process Parameters

The hydrochar properties, including carbon content, density of oxygen-containing functional groups, surface area, porosity, yield, and HHV, are determined by a combination of controllable process parameters. While temperature has the most profound effect on hydrochar properties, followed by residence time, S:L ratio, feedstock composition, and pH, a detailed understanding of how each parameter influences hydrochar properties is essential for designing appropriate HTC conditions to produce hydrochar precursors for activated carbon synthesis.

3.1 Feedstock composition

The composition of the biomass used as a feedstock, i.e., the relative amounts of cellulose, hemicellulose, and lignin, along with other constituents like ash, moisture, and extracts, plays a very important role in controlling HTC process outcomes [10]. This effect is independent of, and may be as important as, the HTC process parameters. Lignin content is positively correlated with hydrochar yield and calorific value. Hemicellulose content is positively correlated with the

density of oxygen-containing functional groups. This functional group density plays a very important role when hydrochar is used as a precursor for chemical activation [16,35]. Ash content may be undesirable, as it can dilute the carbon matrix and cause fouling of activating agents. To tailor hydrochar composition, co-HTC, i.e., the simultaneous HTC of two or more different feedstocks, has gained popularity. Hydrochars derived from blends of cellulose-containing agricultural wastes and protein- or lipid-containing wastes, such as sewage sludge, may be enriched in N-containing functional groups [10].

3.2 Temperature

Temperature is the primary control parameter in hydrothermal carbonization reactions. Raising the temperature from 180 to 260 °C increases the extent of carbonization reactions [37–39]. Consequently, this results in increased carbon and decreased hydrogen and oxygen levels. The effect is attributed to more extensive dehydration and decarboxylation reactions at increased temperatures. The effect is illustrated in van Krevelen plots, where increasing temperature shifts hydrochar data points along lines characteristic of increasing coalification extent [40]. Simultaneously, increasing temperature increases the extent of aromatization, which is important for hydrochar stability. However, this increases at the expense of surface density, which is important for functional oxygen-containing surface groups. The effect is important in the context of activated carbon synthesis. Hydrochars produced at lower temperatures (180-220 °C) have more surface functional groups, which act as sites for activating agents [41]. Hydrochars produced at higher temperatures have more aromatic structures, which are more favorable for physical activation. Hydrochar yield decreases with increasing temperature due to greater dissolution in the liquid medium [42]. The hydrochar yield ranges from 45 to 80 wt%. Temperature affects hydrochar surface characteristics. An increase in temperature yields more defined hydrochar microspheres, which are derived from cellulose- and hemicellulose-derived structures.

3.3 Residence time

Residence time is found to qualitatively influence hydrochar properties in a manner like temperature, increasing hydrochar carbon content, reducing oxygen-containing functional groups, and promoting aromatization. However, this effect is less pronounced than the effect of temperature. For most lignocellulosic feedstocks, hydrochar properties change little after the first 0.5-2 hours of reaction time at a given temperature [7]. Moreover, hydrochar properties show little change for residence times greater than 6-8 hours at a given temperature. An

increase in residence time decreases hydrochar yield due to hydrochar dissolution into the liquid medium, without increasing hydrochar carbon content or HHV. For producing hydrochar precursors for activated carbon synthesis, residence times of 4-12 hours at 180-220°C are optimal for maintaining functional group integrity and ensuring hydrochar structural integrity for activation [43].

3.4 Solid-to-liquid ratio

The S:L ratio, defined as the mass of dry feedstock per unit volume of water, governs both the kinetics and thermodynamics of the HTC process. The hydrolysis and dissolution of biomass constituents are more favorable under dilute conditions, i.e., when the S:L ratio is low. This results in a decreased yield of hydrochar but enhances the transfer of carbon and nutrient content into the process liquid [44]. On the other hand, high S:L ratios increase hydrochar yield but may limit carbonization due to mass-transfer limitations and reduced water availability for hydrolysis. In practice, S:L ratios ranging from 1:5 to 1:15 are commonly used. Ratios close to 1:10 are preferred as these provide a reasonable balance between a sufficient reaction medium and process water [11,14]. From an energy-efficiency standpoint, minimizing the S:L ratio, and hence the volume of water to be heated during the HTC process, is desirable, provided hydrochar quality requirements are met.

3.5 pH and catalytic additives

The pH of the initial reaction mixture and the use of acidic or basic catalysts can significantly affect the course of the hydrothermal carbonization process and the properties of the resulting hydrochar [42]. In the case of an acidic environment, the rate of glycosidic bond hydrolysis increases, thereby accelerating the decomposition of the polysaccharide content and the formation of 5-HMF and furfural derivatives [45]. This, in turn, increases the yield of the condensation-derived secondary char content of the hydrochar. In contrast, in the case of a basic environment, lignin and cellulose are separated, and the formation of levulinic acid derivatives is suppressed. The inclusion of nitrogen-containing co-reactants, such as urea and ammonium chloride, in the HTC process enables in situ nitrogen doping of the hydrochar, introducing pyridinic and pyrolic nitrogen functionalities that are beneficial for electrochemical energy storage devices [46]. This additive-assisted HTC process is a highly effective, single-step surface chemistry engineering technique that avoids the need to subsequently introduce heteroatoms.

Table 1. Summary of HTC Process Parameters and Their Effects on Hydrochar Properties

Parameter	Typical range	Effect on yield	Effect on carbon/functional groups	Implication for AC
Temperature	180–260 °C	↓ with ↑T	↑C content, ↓O/H groups, ↑aromatization	Low T (180–220 °C) preferred for chemical activation precursors
Residence time	0.5–24 h	↓ with ↑t (plateau after 6–8 h)	Similar to T but less pronounced	4–12 h optimal; beyond plateau reduces yield without quality gain
Solid-to-liquid ratio	1:5 to 1:15 (g/mL)	↑ with ↑S:L	↑S:L → limited hydrolysis; ↓S:L → more dissolution	1:10 common balance; lower S:L reduces energy cost
Lignin content	15–30 wt% (typical)	↑ with ↑lignin	↑HHV; aromatic primary char formation	High-lignin feedstocks give more stable precursors
Hemicellulose content	15–35 wt% (typical)	↓ (high dissolution)	↑O-functional groups at low T	Beneficial for chemical activation via KOH/H_3PO_4
pH / additives	Acid (pH 2–4) to base (pH 9–12)	Variable	Acid: ↑hydrolysis; Base: ↑depolymerization; N-dopants: ↑N groups	Urea addition enables single-step N-doping for energy storage ACs

4. Activation Methods and Process Optimization

The activation process for hydrochar to produce high-performance activated carbon is highly regulated, transforming denser hydrochar into a highly porous material with a well-developed surface area and surface chemistry [47]. Two different activation processes have been reported for hydrochar activation to produce activated carbons. Chemical activation involves impregnating hydrochar with a chemical reagent and then thermally activating it, whereas physical

activation involves heating hydrochar in an oxidizing atmosphere at high temperatures [48]. Although physical activation is simpler and avoids the use of harmful chemicals, chemical activation is more commonly used to produce hydrothermal carbonization-derived activated carbons, as it yields activated carbons with better surface properties, especially BET surface area and microporous volume [49,50]. In this section, the activation processes for producing activated carbons from hydrothermal chars will be discussed, with a focus on the three most used chemical reagents: KOH, H_3PO_4, and $ZnCl_2$.

4.1 Chemical Activation

Chemical activation is a two-step procedure consisting of impregnation, in which hydrochar is treated with the activating agent either in aqueous or dry form, and activation, in which the impregnated hydrochar is subjected to thermal treatment at 350-900 °C in an inert atmosphere, typically N_2 [27]. During activation, the activating agent participates in a series of chemical reactions, including dehydration, oxidation, intercalation, and gasification, to form the pore structure of activated carbon. The final product, obtained after washing and drying, is called activated carbon. The activating agent influences the role of micropores, mesopores, and surface functional groups in the final properties of activated carbon. The activation parameters, including the activating agent-to-hydrochar ratio, impregnation time and temperature, activation temperature, and activation time, depend on the activating agent and hydrochar and thus require parameter studies for different hydrochar-activating agent pairs.

4.1.1 KOH activation

Potassium hydroxide activation has been the most investigated chemical activation method for HTC-derived hydrochar materials and is widely accepted as the most promising route for producing carbons with exceptional BET surface areas and well-developed microporosity. The activation reaction involves a redox process between KOH and the carbon matrix, occurring in multiple steps at temperatures above 700 °C [27]. The reaction commences with the reaction of the KOH with the carbon matrix, yielding K_2CO_3, K_2O, and H_2 gases, followed by the decomposition of K_2CO_3 and reduction of K_2O to metallic potassium. The metallic potassium, with a boiling point of 759 °C, is intercalated between the emerging layers of the carbon matrix, thereby expanding the interlayer distance and leading to the development of a highly microporous carbon matrix [51]. The CO and CO_2 gases produced in the reaction also contribute to the development of the pore structure through the gasification of the carbon matrix, particularly around the grain boundaries of the aromatic carbon clusters.

The ratio of KOH to hydrochar has a major impact on the textural properties of the activated carbons prepared [24,25]. An increase in the KOH/carbon ratio from 1:1 to 3:1 (w/w) is seen to enhance the BET surface area and the micropore volume, indicating increased etching of the hydrocarbon by redox reactions and gasification [52]. For the hydrocarbon from rice husks, increasing the KOH/carbon ratio from 1:1 to 1:3 increases the BET surface area from 413 m^2/g to 755 m^2/g, with a corresponding increase in the microporous area. However, for ratios of 3:1 to 4:1, the rate of increase in BET surface area slows and may even decrease, as the high KOH content promotes the formation of large pores from micropores, thereby reducing the volume of micropores [53]. The temperature of activation also affects the surface area of activated carbons prepared by the KOH method, which peaks at 700–800 °C for most hydrocarbon precursors, after which it declines due to sintering of the activated carbon framework and loss of KOH vapor during activation [54]. For the date palm waste, the RSM-optimized method for activated carbon preparation identified 700 °C, 1.5 h, and a 3:1 ratio of KOH to C as the optimum, which yielded a CO_2 uptake capacity of 6.71 mmol/g at 0 °C, the highest capacity reported for activated carbons prepared from biomass materials [55].

In a comparative factorial study, agroforestry waste pretreated with HTC were assessed for three activation parameters (agent-to-precursor ratio, dry impregnation time, and activation time) using a 2^3 factorial design. KOH-activated carbons showed iodine numbers up to 1289 mg/g, significantly higher than those for H_3PO_4 activation, albeit at significantly lower mass yield (18-35%). HTC pretreatment at 190 °C reduced the ash content of the precursors and improved the stability and homogeneity of hydrochar, thus increasing activation efficiency [56].

4.1.2 H_3PO_4 activation

The phosphoric acid activation process follows a mechanism quite different from that of KOH activation. Phosphoric acid, H_3PO_4, essentially works as a dehydration catalyst and a chemical spacer, but it is not a redox reagent [47]. During the impregnation process, phosphoric acid helps to hydrolyze the glycosidic and ether linkages of the polysaccharide components of the hydrochar, and the phosphoric acid and its derivatives, i.e., polyphosphoric acids, which form at high temperatures, act as spacers between the layers of the carbon, thereby physically preventing the layers from collapsing and creating a porous structure after the removal of the phosphoric acid during the washing process. The temperature required for the activation of hydrochar by phosphoric acid is considerably lower than that required for the KOH activation process; i.e., the

optimal temperature for the phosphoric acid activation of hydrochar ranges from 350 to 500 °C, which is quite favorable from an energy and economic standpoint.

Phosphoric acid activation is particularly effective for hydrochar obtained from lignocellulosic biomass, as the inherent structures of plant cell walls, which form the biomass, can act as a matrix for efficient absorption of phosphoric acid during impregnation. Studies were conducted on the phosphoric acid activation of hydrochar obtained from corn cob residue, and the results indicated that the BET surface area increased from 5.69 m^2/g to 2192 m^2/g, and the total pore volume increased from 0.136 to 1.269 cm^3/g at 400 °C and a phosphoric acid to hydrocarbon ratio of 3, i.e., more than 380 times, while maintaining a mesoporous structure, which is quite efficient for the adsorption of large molecules [57]. The pore size distribution of H_3PO_4-activated carbons is also typically broader and more heterogeneous than that of KOH-activated carbons due to the physicochemical differences in the underlying activation processes.

The impregnation ratio and activation temperatures have a significant bearing on the pore characteristics of H_3PO_4-activated carbons. For a constant activation temperature of 400 °C, the surface area and pore volume increase progressively with increasing H_3PO_4-to-hydrochar ratio from 1.5 to 3. However, beyond this ratio, the increase in surface area and pore volume is much smaller due to excessive acid, which tends to corrode the surface and compromise the integrity of the macro-pore structure [58]. Temperatures above 500 °C cause the progressive volatilization of phosphorus and the gradual loss of the characteristic template-induced micro-pore structure. This leads to a gradual loss in surface area. This points to the need for precise control of the activation temperature for H_3PO_4 [47]. In addition, the need to wash the carbons in a dilute NaOH solution to remove impregnated phosphorus species underscores the importance of thorough washing to remove surface contamination and ensure proper adsorptive properties.

4.1.3 $ZnCl_2$ activation

The activation of zinc chloride occupies a mechanistic activation site between the purely redox-based activation of KOH and the template-based activation of H_3PO_4. $ZnCl_2$ activates as a Lewis acid, accelerating dehydration and aromatization reactions in the carbon precursor, and also serves as a template in the activation process, with molten $ZnCl_2$ (melting point 283 °C) occupying the pore volume of the carbon matrix during activation and then being removed by acid washing to leave a ‘negative template’ of the pore structure [59]. This contrasts with KOH activation, which activates carbon by inducing porosity through chemical etching and intercalation, whereas $ZnCl_2$ activates carbon by

occupying pore volume that remains after the $ZnCl_2$ is removed. This results in the pore size distribution of $ZnCl_2$-activated carbons being more mesoporous than that of KOH-activated carbons, with a broader range that includes both micropores and small mesopores [29].

The activation temperature for $ZnCl_2$ is generally within the range of 400-600 °C. At temperatures below 400 °C, biomass activation is incomplete, and at temperatures above 600 °C, volatilization of $ZnCl_2$ occurs because it has a boiling point of 732 °C, leading to loss of the template agent and consequently a decrease in pore volume. The $ZnCl_2$-to-carbon ratio is critical for achieving a balance between microporous and mesoporous development [50]. The 1:1 ratio yields an 80% increase in mesoporous surface area relative to unactivated hydrochar, and ratios greater than 2:1 or 3:1 lead to reduced mesoporous development due to coalescence. For polypyrrole-derived carbons, a 3:1 $ZnCl_2$ to carbon ratio at 600 °C gave the best results for microporous surface area, 1105 m^2/g, and a microporous volume fraction of 86.26%, thus proving that $ZnCl_2$ activation is not only dependent on the hydrochar but also on the precursor material [60].

One drawback of $ZnCl_2$ activation is the environmental impact of zinc-containing effluent streams. Zinc is a regulated heavy metal, and acid wash liquor is a byproduct of $ZnCl_2$ activation and subsequent washing. Zinc recycling and recovery methods have been proposed to alleviate this problem [61].

4.2 Physical Activation

The process of physical activation involves gasifying pre-carbonized hydrochar with an oxidizing gas, typically steam (H_2O) or carbon dioxide (CO_2), at temperatures between 700 and 950 °C [29]. The activating gas reacts with the carbon matrix via endothermic gasification reactions, thereby preferentially removing less-ordered carbon atoms and developing the pore structure from the surface inward. In biomass, physical activation is a two-stage process. The first stage involves carbonization of the raw material, which, in this study, is HTC of the raw biomass. The advantages of physical activation over chemical activation are its simplicity, i.e., no need for washing, and no chemical waste is generated [62]. This process can be used to produce food-grade and pharmaceutical-grade activated carbons when high purity is required. However, physical activation always yields activated carbons with significantly lower BET surface areas and greater microporosity than those produced by chemical activation. Furthermore, the burn-off level required to achieve satisfactory porosity results in substantial mass loss (typically 30-60 wt%).

With respect to HTC-derived hydrochar, physical activation by CO_2 has been demonstrated to produce materials with surface areas ranging from 400 to 800

m^2/g, depending on the temperature of activation and burn-off level, while optimization of the KOH activation process can produce materials with surface areas ranging from 1000 to 3500 m^2/g [63]. The relatively low level of graphitization of hydrochar, along with its high content of reactive oxygen-containing functional groups, renders the material more reactive during physical activation than conventional biochar, enabling the formation of similar porous structures at slightly lower activation temperatures.

5. Applications

Activated carbons prepared via HTC have been examined across a broad range of applications, among which water treatment and electrochemical energy storage are the two that have received the greatest attention and hold the greatest technological relevance. In both domains, the unique combination of surface chemistry, porosity, and eco-friendliness of HTC-derived materials offers competitive, and in some cases superior, performance to conventional activated carbons prepared from coal.

In water treatment, the high density of oxygen-containing surface functional groups, including carboxyl, hydroxyl, and carbonyl, provided by the HTC process, enables strong electrostatic and hydrogen-bond-based interactions for the removal of cationic and anionic contaminants, respectively. For example, co-hydrothermal carbonization of garden waste and sewage sludge increased the methylene blue adsorption capacity to 52.39 mg/g, a 22.6% enhancement over the hydrochar prepared from a single hydrocarbon source, attributed to increased oxygen-containing surface functional groups resulting from lignin decomposition in the sewage sludge [64]. The surface functionalization of wheat straw hydrochar with 3-Aminopropyl triethoxysilane increased the Langmuir adsorption capacity to 49.6 mg/g for Pb(II) and 31.7 mg/g for methylene blue, enhancements of 8.5 and 1.3 times over the unmodified hydrochar, respectively, demonstrating the synergetic effects of combining the HTC method with surface modification for improved water treatment applications [65]. For the removal of heavy metals, the introduction of nitrogen-based surface functional groups via doping of hydrochar materials can enhance the Lewis basic site-based coordination capacity by 2-5 times, and regeneration studies have shown that most hydrochar-based adsorbents retain more than 75% of the original adsorption capacity after four to six cycles, a critical factor for the practical application of hydrochar-based adsorbents for water purification [66].

In the field of electrochemical energy storage devices, activated carbons produced by hydrothermal carbonization have shown promising properties as active materials for electrical double-layer capacitors, where charge storage

capability is determined by surface area and surface conductivity. The low degree of graphitization in hydrochars, compared to pyrolysis-produced biochars, enables the incorporation of heteroatoms and the formation of micro- and mesoporous networks in the final product [46]. Activated carbons produced by KOH, H_3PO_4, and NaOH activation of biomass-based hydrochars have shown BET surface areas ranging from 1,355 to 3,322 m^2/g and specific capacitances up to 179.4 F/g at a current density of 6.25 A/g [67]. Microwave-assisted HTC of biowaste has also produced activated carbons that showed a specific capacitance of 501.6 F/g at 2 A/g and 84.6% capacitance retention after 10,000 cycles [68].

Apart from the main fields of application, HTC-derived activated carbons have also shown promising properties for CO_2 capture in micropore-rich configurations and for the transesterification of vegetable oils to biodiesel using heterogeneous catalysts in the form of sulfonic acid-functionalized activated carbons [7,69]. In addition, HTC-derived activated carbons have also shown promising properties as soil amendment agents [70]. In all of the mentioned fields of application, the performance of HTC-derived activated carbons is ultimately determined by the match between the properties of the porous and surface chemical structure of the final product and the specific physicochemical demands of the respective process, highlighting the importance of the integrated and process-optimization-oriented approach to HTC-derived activated carbon synthesis that has been emphasized throughout this chapter.

6. Challenges & Future

Despite substantial advances in hydrothermally carbonized activated carbons, various interrelated obstacles continue to impede progress towards commercialization. These obstacles range from technical to economic and legal considerations and will ultimately dictate the pace at which hydrothermal carbons replace traditional fossil-derived carbons in commercial applications.

Scale-up is currently considered to be the most pressing technical limitation. While hydrothermal carbonization is typically performed at a laboratory scale in sealed batch autoclaves, scale-up to continuous-flow reactors will require consideration of temperature gradients, corrosion from organic acids under high pressure, and feedstock handling, which may not be concerns at a laboratory scale [41].

The process water management aspect is a critical, often overlooked challenge and cannot be discharged untreated. Valorization of the water, either through anaerobic digestion, nutrient recovery, or controlled recirculation, is technically feasible but increases process complexity and capital costs [71,72]. In activation, the large-scale use of KOH creates corrosive alkaline wastewater, whereas $ZnCl_2$

produces zinc-based wastewater subject to heavy metal discharge regulations. In both cases, chemical recovery infrastructure has important cost implications [73]. Lastly, the lack of standardization in the water characterization protocols in the HTC literature, varying BET degassing conditions, different pore volume reporting conventions, and different adsorption tests make it impossible to compare the performance of different HTC-based ACs and obtain regulatory certification for the use of HTC-based ACs in critical applications like drinking water treatment and pharmaceutical industry applications [74].

Looking forward, the opportunity with the greatest transformative potential lies in the integration of the HTC-based AC production process with the circular bio-economy concept, in which all process streams are valorized simultaneously and data-driven optimization techniques like machine learning, digital twins, and hybrid ML-LCA are employed to bridge the gap between the performance of the process in the laboratory and the reliability of the process in the plant.

7. Conclusions

The HTC process is a technically viable and resource-efficient method for converting wet lignocellulosic materials into activated carbon precursors, thereby eliminating the energy-intensive drying step inherent in other thermochemical conversion approaches. The hydrochar properties, and hence the activated carbon, result from a complex interplay among HTC process parameters, with temperature being the most critical, followed by residence time, solid-to-liquid ratio, and biomass composition. Lower hydrothermal temperatures, i.e., between 180°C and 220°C, help retain oxygen-containing surface functional groups, which enhance the subsequent chemical activation, especially by KOH, which generally results in the highest BET surface areas, above 1000 m^2/g, under optimum reaction conditions. The use of H_3PO_4 as the activating agent offers a lower temperature and more energy-efficient alternative, which results in materials with a wider mesopore size distribution, while $ZnCl_2$ offers a viable compromise between microporosity and mesoporosity, as obtained by physical activation, which, although simpler and cleaner, is limited by the surface area achievable.

In all the application areas studied, i.e., water treatment, electrochemical energy storage, CO_2 capture, and catalysis, the performance of the activated carbons obtained by the HTC process is dictated by the match between the pore and surface chemistry of the materials and the physicochemical requirements of the target application, which emphasizes the importance of a holistic, process-oriented approach, as opposed to optimizing the HTC and subsequent steps independently of each other. Despite the progress made, some challenges have to

be overcome for the large-scale applicability of the HTC process to become a reality, including the scaling-up of the reactors, the management of the process water, the recovery of the chemicals, and the lack of a standardized characterization procedure to allow for a more informed comparison of the results from different research groups, which should be the preferred pathway for the research to be done in the near future, within a framework of a circular bioeconomy, and with the help of data-based optimization tools.

References

[1] Giganti P, Falcone PM. Unveiling latent topics in the interplay of Circular Economy and Energy Transition: A Topic Modelling approach. Resour Conserv Recycl 2025;219:108318. https://doi.org/10.1016/j.resconrec.2025.108318.

[2] Uchimiya M, Wartelle LH, Klasson KT, Fortier CA, Lima IM. Influence of Pyrolysis Temperature on Biochar Property and Function as a Heavy Metal Sorbent in Soil. J Agric Food Chem 2011;59:2501–10. https://doi.org/10.1021/jf104206c.

[3] Lee J, Kim K-H, Kwon EE. Biochar as a Catalyst. Renewable and Sustainable Energy Reviews 2017;77:70–9. https://doi.org/10.1016/j.rser.2017.04.002.

[4] Kambo HS, Dutta A. A comparative review of biochar and hydrochar in terms of production, physico-chemical properties and applications. Renewable and Sustainable Energy Reviews 2015;45:359–78. https://doi.org/10.1016/j.rser.2015.01.050.

[5] Nayak A, Bhushan B, Gupta V, Sharma P. Chemically activated carbon from lignocellulosic wastes for heavy metal wastewater remediation: Effect of activation conditions. J Colloid Interface Sci 2017;493:228–40. https://doi.org/10.1016/j.jcis.2017.01.031.

[6] Marrakchi F, Ahmed MJ, Khanday WA, Asif M, Hameed BH. Mesoporous-activated carbon prepared from chitosan flakes via single-step sodium hydroxide activation for the adsorption of methylene blue. Int J Biol Macromol 2017;98:233–9. https://doi.org/10.1016/j.ijbiomac.2017.01.119.

[7] Başakçılardan Kabakcı S, Karakurt Çevik B, Borand MN, Al K. Hydrochar-derived activated carbons from poplar and spruce sawdust: synthesis, characteristics and carbon adsorption performance. Adsorption 2024;30:2083–98. https://doi.org/10.1007/s10450-024-00542-y.

[8] Ma P, Yang J, Xing X, Weihrich S, Fan F, Zhang X. Isoconversional kinetics and characteristics of combustion on hydrothermally treated biomass. Renew Energy 2017;114:1069–76. https://doi.org/10.1016/j.renene.2017.07.115.

[9] Nakason K, Panyapinyopol B, Kanokkantapong V, Viriya-empikul N, Kraithong W, Pavasant P. Characteristics of hydrochar and hydrothermal liquid products from hydrothermal carbonization of corncob. Biomass Convers Biorefin 2018;8:199–210. https://doi.org/10.1007/s13399-017-0279-1.

[10] Xiao L-P, Shi Z-J, Xu F, Sun R-C. Hydrothermal carbonization of lignocellulosic biomass. Bioresour Technol 2012;118:619–23. https://doi.org/10.1016/j.biortech.2012.05.060.

[11] Liu X, Peng L, Deng P, Xu Y, Wang P, Tan Q, et al. Co-hydrothermal carbonization of sewage sludge and rice straw to improve hydrochar quality: Effects of mixing ratio and hydrothermal temperature. Bioresour Technol 2025;415:131665. https://doi.org/10.1016/j.biortech.2024.131665.

[12] Yoshimoto S, Luthfi N, Nakano K, Fukushima T, Takisawa K. Effects of potassium on hydrothermal carbonization of sorghum bagasse. Bioresour Bioprocess 2023;10:24. https://doi.org/10.1186/s40643-023-00645-4.

[13] dos Santos Rocha MSR, Pratto B, de Sousa R, Almeida RMRG, Cruz AJG da. A kinetic model for hydrothermal pretreatment of sugarcane straw. Bioresour Technol 2017;228:176–85. https://doi.org/10.1016/j.biortech.2016.12.087.

[14] Mendoza Martinez CL, Sermyagina E, Saari J, Silva de Jesus M, Cardoso M, Matheus de Almeida G, et al. Hydrothermal carbonization of lignocellulosic agro-forest based biomass residues. Biomass Bioenergy 2021;147:106004. https://doi.org/10.1016/j.biombioe.2021.106004.

[15] Zhang Z, Zhu Z, Shen B, Liu L. Insights into biochar and hydrochar production and applications: A review. Energy 2019;171:581–98. https://doi.org/10.1016/j.energy.2019.01.035.

[16] Masoumi S, Borugadda VB, Nanda S, Dalai AK. Hydrochar: A Review on Its Production Technologies and Applications. Catalysts 2021;11:939. https://doi.org/10.3390/catal11080939.

[17] Wang T, Zhai Y, Zhu Y, Li C, Zeng G. A review of the hydrothermal carbonization of biomass waste for hydrochar formation: Process conditions, fundamentals, and physicochemical properties. Renewable and Sustainable Energy Reviews 2018;90:223–47. https://doi.org/10.1016/j.rser.2018.03.071.

[18] Satira A, Paone E, Bressi V, Iannazzo D, Marra F, Calabrò PS, et al. Hydrothermal Carbonization as Sustainable Process for the Complete Upgrading of Orange Peel Waste into Value-Added Chemicals and Bio-Carbon Materials. Applied Sciences 2021;11:10983. https://doi.org/10.3390/app112210983.

[19] Ischia G, Fiori L. Hydrothermal Carbonization of Organic Waste and Biomass: A Review on Process, Reactor, and Plant Modeling. Waste Biomass Valorization 2021;12:2797–824. https://doi.org/10.1007/s12649-020-01255-3.

[20] Djandja OS, Liew RK, Liu C, Liang J, Yuan H, He W, et al. Catalytic hydrothermal carbonization of wet organic solid waste: A review. Science of The Total Environment 2023;873:162119. https://doi.org/10.1016/j.scitotenv.2023.162119.

[21] Senthil R. Hydrothermal carbonization materials of leather and paper mill sludge for solid biofuel applications. J Anal Appl Pyrolysis 2025;186:106976. https://doi.org/10.1016/j.jaap.2025.106976.

[22] Libra JA, Ro KS, Kammann C, Funke A, Berge ND, Neubauer Y, et al. Hydrothermal carbonization of biomass residuals: a comparative review of the chemistry, processes and applications of wet and dry pyrolysis. Biofuels 2011;2:71–106. https://doi.org/10.4155/bfs.10.81.

[23] Greco G, Canevesi RLS, Di Stasi C, Celzard A, Fierro V, Manyà JJ. Biomass-derived carbons physically activated in one or two steps for CH4/CO2 separation. Renew Energy 2022;191:122–33. https://doi.org/10.1016/j.renene.2022.04.035.

[24] Qi X, Jin L, Gao S, Zhu Z. Carbonization of rice husk in an oxygen-limited counter-current combustion and KOH activation of the biochar. Biomass Bioenergy 2025;193:107599. https://doi.org/10.1016/j.biombioe.2025.107599.

[25] Kaewtrakulchai N, Chanpee S, Jadsadajerm S, Wongrerkdee S, Manatura K, Eiad-Ua A. Co-hydrothermal carbonization of polystyrene waste and maize stover combined with KOH activation to develop nanoporous carbon as catalyst support for catalytic hydrotreating of palm oil. Carbon Resources Conversion 2024;7:100231. https://doi.org/10.1016/j.crcon.2024.100231.

[26] Gao Y, Yue Q, Gao B, Li A. Insight into activated carbon from different kinds of chemical activating agents: A review. Science of the Total Environment 2020;746. https://doi.org/10.1016/j.scitotenv.2020.141094.

[27] Njoku VO, Foo KY, Asif M, Hameed BH. Preparation of activated carbons from rambutan (Nephelium lappaceum) peel by microwave-induced KOH activation for acid yellow 17 dye adsorption. Chemical Engineering Journal 2014;250:198–204. https://doi.org/10.1016/j.cej.2014.03.115.

[28] Phiri J, Ahadian H, Sandberg M, Granström K, Maloney T. The Influence of Physical Mixing and Impregnation on the Physicochemical Properties of Pine Wood Activated Carbon Produced by One-Step ZnCl2 Activation. Micromachines (Basel) 2023;14:572. https://doi.org/10.3390/mi14030572.

[29] Şahin Ö, Saka C, Ceyhan AA, Baytar O. Preparation of High Surface Area Activated Carbon from *Elaeagnus angustifolia* Seeds by Chemical Activation with $ZnCl_2$ in One-Step Treatment and its Iodine Adsorption. Sep Sci Technol 2015;50:886–91. https://doi.org/10.1080/01496395.2014.966204.

[30] Kumari R, Singh A, Sharma R, Malaviya P. Conversion of food waste into energy and value-added products: a review. Environ Chem Lett 2024;22:1759–90. https://doi.org/10.1007/s10311-024-01742-2.

[31] Wu S, Wang Q, Fang M, Wu D, Cui D, Pan S, et al. Hydrothermal carbonization of food waste for sustainable biofuel production: Advancements, challenges, and future prospects. Science of The Total Environment 2023;897:165327. https://doi.org/10.1016/j.scitotenv.2023.165327.

[32] Ighalo JO, Akaeme FC, Georgin J, de Oliveira JS, Franco DSP. Biomass Hydrochar: A Critical Review of Process Chemistry, Synthesis Methodology, and Applications. Sustainability 2025;17:1660. https://doi.org/10.3390/su17041660.

[33] Tekin K, Karagöz S, Bektaş S. A review of hydrothermal biomass processing. Renewable and Sustainable Energy Reviews 2014;40:673–87. https://doi.org/10.1016/j.rser.2014.07.216.

[34] Peterson AA, Vogel F, Lachance RP, Fröling M, Antal Jr, MJ, Tester JW. Thermochemical biofuel production in hydrothermal media: A review of sub- and supercritical water technologies. Energy Environ Sci 2008;1:32. https://doi.org/10.1039/b810100k.

[35] Peter Z. Order in cellulosics: Historical review of crystal structure research on cellulose. Carbohydr Polym 2021;254:117417. https://doi.org/10.1016/j.carbpol.2020.117417.

[36] Lucian M, Volpe M, Gao L, Piro G, Goldfarb JL, Fiori L. Impact of hydrothermal carbonization conditions on the formation of hydrochars and secondary chars from the organic fraction of municipal solid waste. Fuel 2018;233:257–68. https://doi.org/10.1016/j.fuel.2018.06.060.

[37] Becker R, Dorgerloh U, Paulke E, Mumme J, Nehls I. Hydrothermal Carbonization of Biomass: Major Organic Components of the Aqueous Phase. Chem Eng Technol 2014;37:511–8. https://doi.org/10.1002/ceat.201300401.

[38] Wang T, Zhai Y, Zhu Y, Peng C, Xu B, Wang T, et al. Influence of temperature on nitrogen fate during hydrothermal carbonization of food waste. Bioresour Technol 2018;247:182–9. https://doi.org/10.1016/j.biortech.2017.09.076.

[39] Liu F, Yu R, Ji X, Guo M. Hydrothermal carbonization of holocellulose into hydrochar: Structural, chemical characteristics, and combustion behavior. Bioresour Technol 2018;263:508–16. https://doi.org/10.1016/j.biortech.2018.05.019.

[40] Heidari M, Dutta A, Acharya B, Mahmud S. A review of the current knowledge and challenges of hydrothermal carbonization for biomass conversion. Journal of the Energy Institute 2019;92:1779–99. https://doi.org/10.1016/j.joei.2018.12.003.

[41] Vu TM, Phuong Nguyen TM, Van H-T, Le NT, Tran D-T. Biomass-derived hydrochar and activated carbon in pharmaceutical pollution mitigation: a comprehensive overview. RSC Adv 2025;15:43053–84. https://doi.org/10.1039/D5RA04857E.

[42] Zhang Y, Jiang Q, Xie W, Wang Y, Kang J. Effects of temperature, time and acidity of hydrothermal carbonization on the hydrochar properties and nitrogen recovery from corn stover. Biomass Bioenergy 2019;122:175–82. https://doi.org/10.1016/j.biombioe.2019.01.035.

[43] Lin Y, Xu H, Gao Y, Zhang X. Preparation and characterization of hydrochar-derived activated carbon from glucose by hydrothermal carbonization. Biomass Convers Biorefin 2023;13:3785–96. https://doi.org/10.1007/s13399-021-01407-y.

[44] Si H, Zhao C, Wang B, Liang X, Gao M, Jiang Z, et al. Liquid-solid ratio during hydrothermal carbonization affects hydrochar application potential in soil: Based on characteristics comparison and economic benefit analysis. J Environ Manage 2023;335:117567. https://doi.org/10.1016/j.jenvman.2023.117567.

[45] Fakudze S, Wei Y, Zhou P, Han J, Chen J. Synergistic effects of process-generated organic acids during co-hydrothermal carbonization of watermelon peel and high-sulfur coal. J Environ Chem Eng 2022;10:107519. https://doi.org/10.1016/j.jece.2022.107519.

[46] Prieto M, Yue H, Brun N, Ellis GJ, Naffakh M, Shuttleworth PS. Hydrothermal Carbonization of Biomass for Electrochemical Energy Storage: Parameters, Mechanisms, Electrochemical Performance, and the Incorporation of Transition Metal Dichalcogenide Nanoparticles. Polymers (Basel) 2024;16:2633. https://doi.org/10.3390/polym16182633.

[47] Liu Q-S, Zheng T, Wang P, Guo L. Preparation and characterization of activated carbon from bamboo by microwave-induced phosphoric acid activation. Ind Crops Prod 2010;31:233–8. https://doi.org/10.1016/j.indcrop.2009.10.011.

[48] Ao W, Fu J, Mao X, Kang Q, Ran C, Liu Y, et al. Microwave assisted preparation of activated carbon from biomass: A review. Renewable and Sustainable Energy Reviews 2018;92:958–79. https://doi.org/10.1016/j.rser.2018.04.051.

[49] Sulaiman NS, Hashim R, Mohamad Amini MH, Danish M, Sulaiman O. Optimization of activated carbon preparation from cassava stem using response surface methodology on surface area and yield. J Clean Prod 2018;198:1422–30. https://doi.org/10.1016/j.jclepro.2018.07.061.

[50] Moralı U, Demiral H, Şensöz S. Optimization of activated carbon production from sunflower seed extracted meal: Taguchi design of experiment approach and analysis of variance. J Clean Prod 2018;189:602–11. https://doi.org/10.1016/j.jclepro.2018.04.084.

[51] Illingworth JM, Rand B, Williams PT. Understanding the mechanism of two-step, pyrolysis-alkali chemical activation of fibrous biomass for the production of activated carbon fibre matting. Fuel Processing Technology 2022;235:107348. https://doi.org/10.1016/j.fuproc.2022.107348.

[52] Petrovic B, Gorbounov M, Masoudi Soltani S. Influence of surface modification on selective CO2 adsorption: A technical review on mechanisms and methods. Microporous and Mesoporous Materials 2021;312:110751. https://doi.org/10.1016/j.micromeso.2020.110751.

[53] Nandi R, Jha MK, Guchhait SK, Sutradhar D, Yadav S. Impact of KOH Activation on Rice Husk Derived Porous Activated Carbon for Carbon Capture at Flue Gas alike Temperatures with High CO_2 /N_2 Selectivity. ACS Omega 2023;8:4802–12. https://doi.org/10.1021/acsomega.2c06955.

[54] Dziejarski B, Serafin J, Hernández-Barreto DF, Naumovska E, Sreńscek-Nazzal J, Klomkliang N, et al. Tailoring highly surface and microporous activated carbons (ACs) from biomass via KOH, $K_2C_2O_4$ and KOH/K2C2O4 activation for efficient CO_2 capture and CO2/N2 selectivity: characterization, experimental and molecular simulation insights. Chemical Engineering Journal 2025;524:169677. https://doi.org/10.1016/j.cej.2025.169677.

[55] Al-Ghurabi EH, Boumaza MM, Al-Masry W, Asif M. Optimizing the synthesis of nanoporous activated carbon from date-palm waste for enhanced CO2 capture. Sci Rep 2025;15:17132. https://doi.org/10.1038/s41598-025-00498-1.

[56] Vallejo F, Yánez D, Díaz-Robles L, Oyaneder M, Alejandro-Martín S, Zalakeviciute R, et al. Valorizing Biomass Waste: Hydrothermal Carbonization and Chemical Activation for Activated Carbon Production. Biomass 2025;5:45. https://doi.org/10.3390/biomass5030045.

[57] Chen J, Zhang L, Yang G, Wang Q, Li R, Lucia LA. Preparation and Characterization of Activated Carbon from Hydrochar by Phosphoric Acid Activation and its Adsorption Performance in Prehydrolysis Liquor. Bioresources 2017;12. https://doi.org/10.15376/biores.12.3.5928-5941.

[58] Nakason K, Phanthuwongpakdee J, Youngjan S, Kraithong W, Phanthasri J, Toomsan W, et al. Unraveling catalytic conversion of spent coffee grounds through alkaline and alkaline earth metal phosphates in hydrothermal carbonization. Fuel 2024;372:132233. https://doi.org/10.1016/j.fuel.2024.132233.

[59] Li B, Li C, Li D, Zhang L, Zhang S, Cui Z, et al. Activation of pine needles with zinc chloride: Evolution of functionalities and structures of activated carbon versus increasing temperature. Fuel Processing Technology 2023;252:107987. https://doi.org/10.1016/j.fuproc.2023.107987.

[60] Li B, Hu J, Xiong H, Xiao Y. Application and Properties of Microporous Carbons Activated by $ZnCl_2$: Adsorption Behavior and Activation Mechanism. ACS Omega 2020;5:9398–407. https://doi.org/10.1021/acsomega.0c00461.

[61] Bosch D, Back JO, Gurtner D, Giberti S, Hofmann A, Bockreis A. Alternative feedstock for the production of activated carbon with ZnCl2: Forestry residue biomass and waste wood. Carbon Resources Conversion 2022;5:299–309. https://doi.org/10.1016/j.crcon.2022.09.001.

[62] Pereira L, Calero M, Blázquez G, González-Egido S, González-Lucas M, Martín-Lara MÁ, et al. On the physical activation of biomass and urban waste chars for water treatment and CO2 adsorption. Chem Eng Sci 2025;313:121749. https://doi.org/10.1016/j.ces.2025.121749.

[63] Khuong DA, Nguyen HN, Tsubota T. Activated carbon produced from bamboo and solid residue by CO2 activation utilized as CO2 adsorbents. Biomass Bioenergy 2021;148:106039. https://doi.org/10.1016/j.biombioe.2021.106039.

[64] Wu C, Zhao Z, Zhong J, Lv Y, Yan X, Wu Y, et al. Adsorption of dye through hydrochar derived from co-hydrothermal carbonization of garden waste and sewage sludge: The adsorption enhancement mechanism of lignin component. Journal of Water Process Engineering 2024;67:106233. https://doi.org/10.1016/j.jwpe.2024.106233.

[65] Zhang Y, Wan Y, Zheng Y, Yang Y, Huang J, Chen H, et al. Hydrochar Loaded with Nitrogen-Containing Functional Groups for Versatile Removal of Cationic and Anionic Dyes and Aqueous Heavy Metals. Water (Basel) 2024;16:3387. https://doi.org/10.3390/w16233387.

[66] Yu W, Lian F, Cui G, Liu Z. N-doping effectively enhances the adsorption capacity of biochar for heavy metal ions from aqueous solution. Chemosphere 2018;193:8–16. https://doi.org/10.1016/j.chemosphere.2017.10.134.

[67] Ding L, Zou B, Li Y, Liu H, Wang Z, Zhao C, et al. The production of hydrochar-based hierarchical porous carbons for use as electrochemical supercapacitor electrode materials. Colloids Surf A Physicochem Eng Asp 2013;423:104–11. https://doi.org/10.1016/j.colsurfa.2013.02.003.

[68] Duraisamy N, Shenniangirivalasu Kandasamy K, Dhandapani E, Kandiah K, Panchu SJ, Swart HC. Biomass Derived 3D Hierarchical Porous Activated

Carbon for Solid-State Symmetric Supercapacitors. J Inorg Organomet Polym Mater 2026;36:546–68. https://doi.org/10.1007/s10904-025-03837-x.

[69] Fadhil AB, Dheyab MM, Abdul-Qader A-QY. Purification of biodiesel using activated carbons produced from spent tea waste. Journal of the Association of Arab Universities for Basic and Applied Sciences 2012;11:45–9. https://doi.org/10.1016/j.jaubas.2011.12.001.

[70] Balmuk G, Cay H, Duman G, Kantarli IC, Yanik J. Hydrothermal carbonization of olive oil industry waste into solid fuel: Fuel characteristics and combustion performance. Energy 2023;278:127803. https://doi.org/10.1016/j.energy.2023.127803.

[71] Pan S-Y, Lin YJ, Snyder SW, Ma H-W, Chiang P-C. Assessing the environmental impacts and water consumption of pretreatment and conditioning processes of corn stover hydrolysate liquor in biorefineries. Energy 2016;116:436–44. https://doi.org/10.1016/j.energy.2016.09.109.

[72] Kapusta K. Effect of ultrasound pretreatment of municipal sewage sludge on characteristics of bio-oil from hydrothermal liquefaction process. Waste Management 2018;78:183–90. https://doi.org/10.1016/j.wasman.2018.05.043.

[73] Malik SA, Khan S, Dar BA. Removal of Heavy Metal Ions(Fe2+, Mn2+, Cu2+ and Zn2+) on to Activated Carbon Prepared from Kashmiri Walnut Shell (Juglans regia). Universal Journal of Green Chemistry 2024:87–95. https://doi.org/10.37256/ujgc.2120244806.

[74] Ischia G, Berge ND, Bae S, Marzban N, Román S, Farru G, et al. Advances in Research and Technology of Hydrothermal Carbonization: Achievements and Future Directions. Agronomy 2024;14:955. https://doi.org/10.3390/agronomy14050955.